

Investigations of Soot Nucleation and Oxidation in a Micro-flow reactor

A Thesis

Presented to

the faculty of the School of Engineering and Applied Science

University of Virginia

in partial fulfillment

of the requirements for the degree

Master of Science in Mechanical and Aerospace Engineering

by

Kelvin Uyi Efemwenkiele

May
2023

APPROVAL SHEET

The thesis
is submitted in partial fulfillment of the requirements
for the degree of
Master of Science in Mechanical and Aerospace Engineering

Kelvin Uyi Efemwenkiele

Author

The thesis has been read and approved by the examining committee:

Prof. Chloe Dedic

Committee Chairman

Prof. Harsha Chelliah

Advisor

Prof. Lin Ma

Accepted for the School of Engineering and Applied Science:

Dean, School of Engineering and Applied Science

May

2023

ABSTRACT

The emission of particulate matter or soot from gas-turbine engines is a major environmental and health concern globally. The production and oxidation of soot depend on the operating conditions and fuels used in gas-turbine engines. The aim of this study was to investigate the nucleation and growth of soot particles during the oxidation of Jet fuels (traditional and alternate bio-derived) using a micro-flow tube reactor in the laboratory. To achieve this goal, Scanning Mobility Particle Sizer (SMPS) with a nano-differential mobility analyzer and condensation particle counter was used to obtain real-time measurements of nascent soot particles. The particle size distributions (from 3nm to 150 nm) were obtained for a range of reactor temperatures, flow residence times, and species compositions. Specifically, for a pressure of 1 atm, the nominal reactor temperature varied between 1173 to 1323 K while the residence time was varied between 80 to 160ms. The results showed that the particle size distributions during the oxidation of Jet fuels were normally distributed. Additionally, the number density of soot particles increased with increasing flow residence times and with increasing temperature. More importantly, alternate jet fuels containing C10 iso-paraffins and trimethyl benzene showed a much stronger propensity for soot nucleation when compared to C12 and C16 highly branched paraffins. Data obtained from this type of experiment can be used in developing and validating soot nucleation/oxidation models used in CFD simulations of next generation gas-turbine engines with alternate bio-derived Jet fuels.

ACKNOWLEDGEMENTS

My gratitude to my academic mentor and advisor Prof Harsha Chelliah who gave me the opportunity, direction and all the help needed during this program.

I also want to thank my colleagues in the lab for giving the needed support. Special thanks to Matthew Quiram for been my partner all through the troubleshooting days.

I also want to thank my wife and son for being by me throughout the duration of this program.

Table of Contents

| | |
|-----------------------------|----|
| APPROVAL SHEET | ii |
|-----------------------------|----|

| | |
|---|-----|
| ABSTRACT | iii |
| ACKNOWLEDGEMENTS | iv |
| 1.INTRODUCTION | 1 |
| 1.1 Background..... | 1 |
| 1.2 Aim | 3 |
| 1.3 Approach..... | 3 |
| The goal of this study is to measure the soot particle size distribution function (PSDF) in a micro flow tube reactor (MFTR) through the online sampling procedure using the nano-Scanning Mobility Particle Sizer (nano-SMPS)..... | 3 |
| 1.4 Significance of Study..... | 3 |
| 2. LITERATURE REVIEW | 4 |
| 2.1 Introduction | 4 |
| 2.2 Micro Flow Tube Reactors in Combustion Research..... | 5 |
| 2.3 Scope of Literature Review | 7 |
| 2.3.1 Soot Particle Formation and Growth Mechanisms | 7 |
| 2.3.2 Chemical and Physical Process in Soot Particle Formation | 7 |
| 2.4 Effect of Fuel Type, Combustion Conditions, and other Factors on Soot Particle Formation and Growth | 17 |
| 2.5 Experimental Techniques for Measuring Soot Particle Size Distribution | 19 |
| 2.5.1 Experimental Techniques for Soot Particle Size and Concentration | 20 |
| 2.5.2 SMPS Technique for Measuring Soot Particle Size | 25 |
| 2.6 Advantages and Limitations of Experimental and Modeling Method..... | 28 |
| 2.7 Identification of Gaps in Literature and Potential Areas for Future Research | 31 |
| 3. METHODOLOGY | 33 |
| 3.1 Experimental setup | 33 |
| 3.1.1 Set up for Micro flow tube reactor (MFTR)..... | 33 |
| 3.1.2 New high-pressure chamber/reactor | 36 |
| 3.2 Scanning Mobility Particle Sizer | 37 |
| 3.2.1 Mobility Diameter | 42 |
| 3.3 Calibration of Orifice Flow Rate | 42 |
| 3.4 Summary..... | 47 |
| 4. RESULTS AND DISCUSSIONS | 48 |
| 4.1 Novel flow configuration for soot nucleation and oxidation investigations..... | 48 |
| 4.2 Soot Data with Jet A (POSF 10325) Pyrolysis and Oxidation | 49 |
| 4.3 Soot Data with Alternate Jet Fuels C1 (POSF 11498) and C5 (PSOF 12345)..... | 53 |
| 4.4 Summary: Data based on the distinction between C1 and C5..... | 54 |
| 5. CONCLUSION | 55 |

| | |
|-------------------------------|----|
| 5.1 Future works | 56 |
| REFERENCES | 57 |

1.INTRODUCTION

1.1 Background

Combustion is usually referred to as a high temperature exothermic redox chemical reaction between fuel and oxidant, in most cases the oxidant is usually oxygen, which yields gaseous products. It finds application in several fields of human endeavor, amongst which are power generation, manufacturing, transportation material synthesis etc. One vital issue which occurs in combustion is when the combustion is said to be incomplete.

This phenomenon is what produces soot. Soot is said to be a product of incomplete combustion and thus undesirable. Its formation process is very complex, hence, the reason why it's a leading research topic amongst intellectuals (74).

Soot particles are a major contaminant that have a considerable impact on air quality and climate change. As a result, it is critical to forecast the mass, size distribution, and morphology of soot aerosol particles formed during combustion operations. Several physical and chemical phenomena, such as thermo-fluid dynamics, gas-phase and heterogeneous chemical reactions, and aerosol dynamics, interact during soot formation, necessitating a complex investigation procedure to develop mathematical models for these phenomena and validate them by comparing their predictions to measurements.

The characterization of soot particles in micro flow tube reactors is one area of research that has been addressed. These small-scale reactors provide a controlled setting for studying the effect of operational parameters on soot particle production. In general, researchers have used a variety of analytical techniques, including scanning mobility particle size (SMPS), transmission electron microscopy (TEM), scanning electron microscopy (SEM), thermophoretic sampling, and laser-induced sampling. But in this study the tool of interest will be the SMPS.

Scanning mobility particle size analysis is one of the most extensively used methods for determining particle size distribution. It entails utilizing a differential mobility analyzer (DMA) to classify particles based on their electrical mobility, followed by measuring particle number concentration at each size range. This approach has been used to analyze the size distribution of soot particles in micro flow tube reactors. (83) employed SMPS to investigate the effect of reactor temperature and dwell time on soot production and development in a micro flow tube reactor.

However, the problems posed by soot emissions have become of critical concern to the world. The need to control soot emissions in combustion by limiting soot inception of particles and growth is of importance. To better understand soot formation and properties, soot needs to be studied under varying conditions in the bid to develop a viable strategy. Although many different fuels have been studied in time past, focus has not really been given to sustainable aviation fuels such as Jet A, Jet C1 and Jet C5 which are the focus of this research. This study seeks to generate experimental data that can be applied into modelling of combustion systems using such sustainable aviation fuels.

For this research, both pyrolysis and oxidation were employed at different experimental conditions, with a mixture of nitrogen and oxygen even been applied in some cases. Soot oxidation been a process in which oxygen is added to the particulate matter formed as a result of incomplete combustion of fuels in order to break it into CO_2 and H_2O . The reason for this is to reduce the harmful effect of these particulate matters as much as possible, to keep the environment clean. One way this is done is by adding oxygen into the fuel mixture during combustion. Some other studies have achieved this by using oxygenated fuels or by adding an oxygen containing compound to the fuel or air stream. But in this study, oxygen addition will be employed.

1.2 Aim

Two key aims of this investigation:

- soot oxidation on size distribution, and
- soot nucleation with alternate fuels

1.3 Approach

The goal of this study is to measure the soot particle size distribution function (PSDF) in a micro flow tube reactor (MFTR) through the online sampling procedure using the nano-Scanning Mobility Particle Sizer (nano-SMPS).

1.4 Significance of Study

This research is relevant because the measurement of soot PSDF in micro-flow tube reactors (MFTRs) is crucial in understanding and optimizing the combustion processes. MFTRs are extensively utilized in various studies due to their compactness, high efficiency, and low emissions. However, the accurate measurement of soot PSDF in these reactors has been a challenge due to their small size and complex flow dynamics. The use of the nano-Scanning Mobility Particle Sizer (nano-SMPS) to determine the soot PSDF in real-time provides a novel approach to accurately characterizing the PSD and understanding the underlying combustion processes. This study has the potential to contribute to the continuous advancement of cleaner and more efficient combustion technologies with reduced emissions.

2. LITERATURE REVIEW

2.1 Introduction

This literature review will provide a critical assessment of experimental and modeling research, as well as a comprehensive analysis of existing research on soot particle distribution in micro flow tube reactors. The review emphasizes the necessity of investigating soot particle distribution in combustion systems, the dangers that soot poses to both human health and the environment, and the potential benefits of reducing soot emissions. Furthermore, the paper highlighted micro flow tube reactors, a promising technique for enhancing combustion efficiency while decreasing emissions, and lastly described special characteristics and prospective applications in a few industries.

The review will identify knowledge gaps and research needs in this topic by comparing experimental and modeling data, and it will also recommend future research choices for increasing our understanding of soot particle distribution in micro flow tube reactors. The formation and development of soot particles in combustion systems has a significant impact on the efficiency and emissions of these systems, and soot particles are a major contributor to air pollution, which causes global mortality and morbidity (20, 23). Therefore, understanding the behavior of soot particles is critical when developing plans to reduce emissions and enhance energy efficiency in a range of sectors, including transportation, power generation, and industrial sectors (9, 14, 31).

Soot particles are created because of incomplete combustion of hydrocarbon fuels and are made up of a complex blend of carbonaceous particles (54, 77). These particles can vary in size from a few nanometers to several micrometers and can have a major impact on the characteristics and performance of combustion systems (70). According to (99), soot particles in diesel engines reduced fuel efficiency and increased particulate matter emissions, both of which can be harmful to human health and the environment.

Studying soot particle distribution in combustion systems is important for several reasons. Firstly, it improves our understanding of the fundamental mechanisms underlying soot particle formation and growth. This knowledge can be utilized to create accurate models of combustion systems and design more effective techniques for reducing soot emissions (43). Secondly, studying soot particle distribution accelerates technological advancement in the development of advanced diagnostic techniques such as Laser-induced incandescence (LII), transmission electron microscopy (TEM), and Thermophoretic sampling (TS) for measuring and characterizing soot particles in combustion systems (53).

Some of these techniques can monitor the performance of combustion systems in real-time and to detect and diagnose potential problems (79). Finally, conducting research on soot particle distribution can improve the design and expedite the optimization of combustion systems for improved performance and reduced emissions (24). For instance, researchers can design reactors that are more efficient and produce fewer emissions by understanding the factors that influence soot particle distribution in micro flow tube reactors (20).

In conclusion, understanding the behavior of soot particles in combustion systems is critical for improving energy efficiency, reducing emissions, and protecting human health and the environment. Further research in this area is needed to develop more accurate models of combustion systems, advanced diagnostic techniques, and optimized combustion systems for a sustainable future.

2.2 Micro Flow Tube Reactors in Combustion Research

Micro flow tube reactors are a type of reactor that is commonly used in combustion research due to their unique features and advantages. These reactors are distinguished by their compact size and the presence of multiple, parallel channels or tubes through which reactants flow (4). This design allows for precise control over the reaction conditions and enables researchers to study the behavior of different fuels and combustion processes under controlled conditions (87).

One of the key advantages of MFTR is the high surface area-to-volume ratio, which promotes efficient heat transfer and allows for rapid reaction rates. This is significant in combustion research, where accurate measurements of reaction kinetics and product distributions are critical for understanding the underlying mechanisms of combustion processes (13). By using MFTR, researchers can obtain more accurate and precise measurements of these parameters than would be possible with larger-scale reactors (21).

In addition to their high efficiency and precision, MFTR are also highly versatile and applicable in varying combustion processes and fuels (101). For instance, researchers have used these reactors to examine the combustion of hydrocarbon fuels like methane and propane, as well as alternative fuels which includes biofuels and hydrogen (35, 82, 2). The ability to analyze different types of fuels and combustion processes makes micro flow tube reactors a valuable tool for advancing the field of combustion science and developing more efficient and sustainable energy technologies.

Furthermore, micro flow tube reactors are well-suited for investigating the formation and behavior of soot particles in combustion systems, which is an important area of research because of the significant health and environmental impacts associated with soot emissions. Researchers can utilize MFTR to simulate realistic combustion conditions and obtain extensive data on the morphology, size distribution, and chemical composition of soot particles (38). This information is critical for developing more accurate models of soot formation and behavior, which can in turn inform the development of more effective strategies for reducing soot emissions.

Overall, micro flow tube reactors play a critical role in advancing our understanding of combustion processes and developing more efficient and sustainable energy technologies. Their high efficiency, precision, versatility, and ability to study soot particle behavior make them an essential tool for combustion researchers.

2.3 Scope of Literature Review

The scope of this literature review will be limited to studies published in peer-reviewed journals and conference proceedings from the past decade. Both experimental and sectional modeling investigations of soot particle distribution in micro flow tube reactors will be considered, and the review will cover a wide range of fuels and combustion conditions. In addition to providing a comprehensive overview of the current state of knowledge on this topic, this literature review will also identify key research gaps and future directions for further investigation.

2.3.1 Soot Particle Formation and Growth Mechanisms

Soot particle formation and growth in combustion systems are complicated processes that include numerous mechanisms and are affected by a variety of factors or parameters such as fuel mix, temperature, and pressure. This section provides in-depth examinations of the numerous soot particle formation and growth mechanisms, such as, nucleation, surface growth, and coagulation. This section will also discuss how fuel properties, combustion conditions, and reactor design affect the formation and development of soot particles, with an emphasis on important factors affecting the distribution of soot particles in the MFTR.

2.3.2 Chemical and Physical Process in Soot Particle Formation

Soot particles are complex aggregates of carbonaceous components formed during combustion processes, particularly in hydrocarbon fuels. Soot particle generation is an intricate process that combines both chemical and physical processes. Designing more efficient and cleaner combustion systems requires an understanding of the processes that result in the creation of soot particles. The chemical and physical processes that contribute to the formation of soot particles will be discussed in this section.

The nucleation process, which results in the development of small carbon atom clusters known as polycyclic aromatic hydrocarbons, is one of the main mechanisms responsible for soot particle formation (PAHs). Figure 2.1 shows the process of pyrolysis, or the breakdown of fuel molecules into smaller hydrocarbon molecules, which results in the formation of PAHs (32).

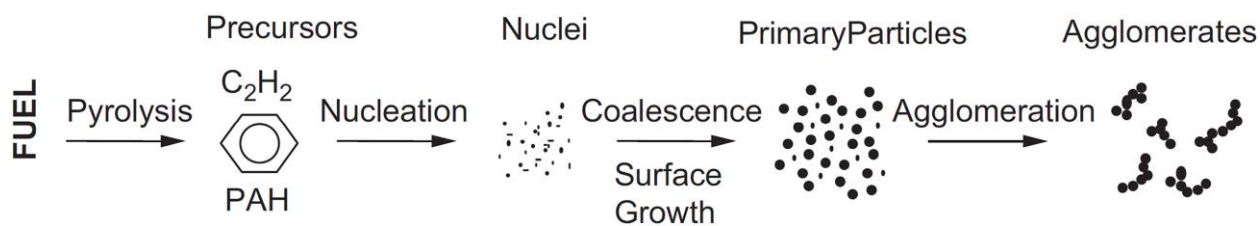


Figure 2.1: Representation of soot formation (32)

The PAHs then undergo further reactions to form stable aromatic compounds. The aromatic compounds condense into small, spherical particles known as primary particles (45, 103). As seen in figure 2.2 (50) utilized PAH structures ranging from 2 aromatic (Naphthalene) rings to 19 aromatic rings (Circumcoronene).

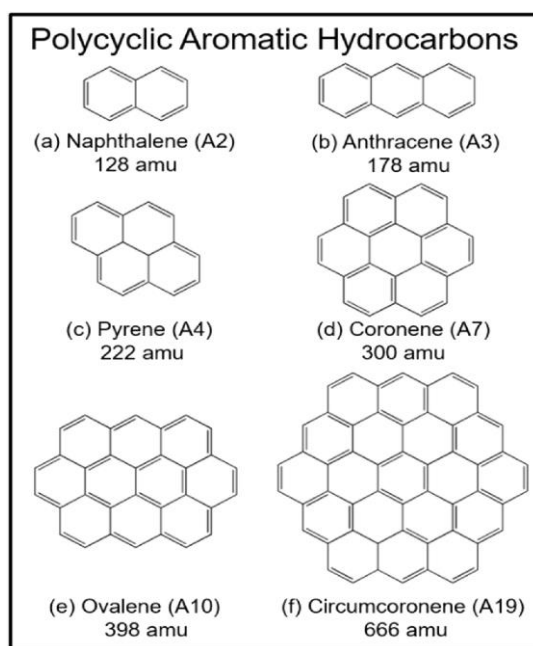


Figure 2.2 Structure of PAH Monomers (50)

After the formation of primary particles, the physical process of surface growth comes into play. During this process, the primary particles grow by absorbing more carbonaceous material onto their surfaces. The formation of soot particles by surface growth is affected by various factors such as fuel composition, temperature, and pressure. The rate of growth of the particles

is also influenced by the concentration of PAHs in the combustion system (32). As the soot particles grow, they become more complex in structure, and this leads to the coagulation process. Coagulation occurs when primary particles collide and stick together, forming larger aggregates. The collision and sticking of particles depend on various factors such as particle size, concentration, and temperature (58).

The chemical and physical processes in soot particle formation and growth are complex and involve multiple mechanisms. The rate of formation and growth of soot particles is influenced by various parameters, including fuel composition, temperature, pressure, and reactor design (61, 86). A thorough understanding of these processes is essential in developing efficient and cleaner combustion systems. Overall, better insight on the physical and chemical processes in soot particle formation and growth is crucial for developing combustion systems that is clean and more efficient. Further research is required to analyze the effects of various parameters on soot particle formation and growth in micro flow tube reactors.

2.3.3 Mechanisms of Soot Particle Growth

The growth of soot particles in combustion systems occurs through different mechanisms, including nucleation, coagulation, and surface growth. These mechanisms are described in depth in this section since understanding them is critical for developing successful solutions to reduce soot emissions in combustion systems.

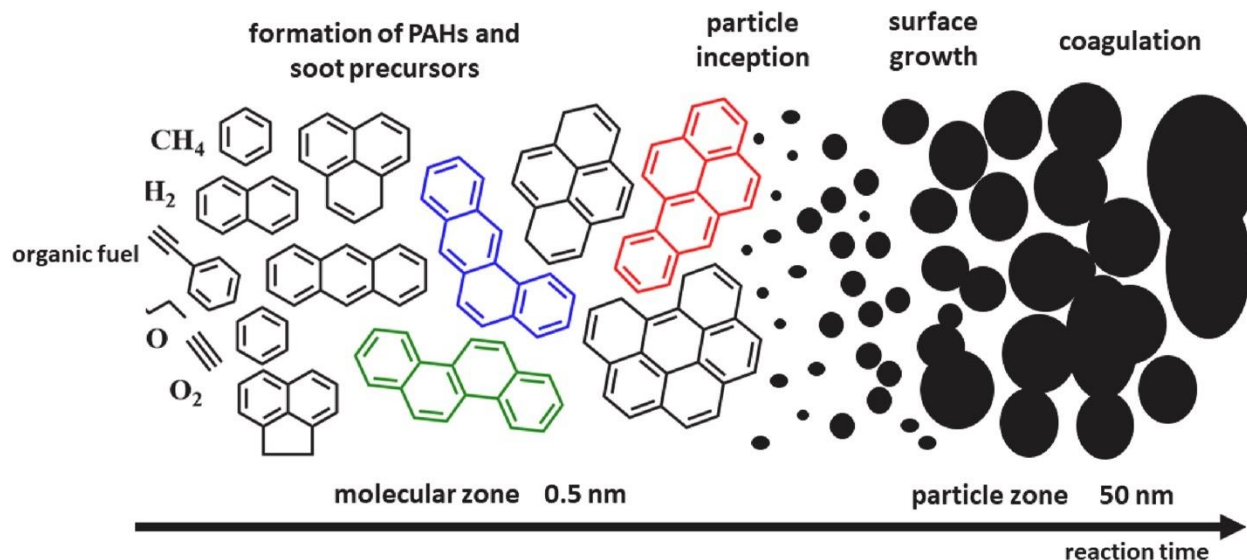


Figure 2.3: Schematic representation of soot formation by (68)

2.3.3.1 Nucleation

Nucleation is the initial process by which small molecules or clusters combine to form a larger particle. In the case of soot, nucleation occurs through the development of polycyclic aromatic hydrocarbons (PAHs) from the decomposition of fuel. These PAHs then undergo condensation to form small particles, which eventually grow into larger soot particles (50). PAHs are formed through a complex network of chemical reactions involving intermediate species, such as radicals and aromatic compounds (43).

The formation of PAHs and their subsequent condensation into small particles are a result of factors, such as fuel composition, pressure, and temperature. The fuel's chemical composition is an important factor that determines the amount and types of PAHs formed during the combustion process. The role of fuel composition in defining the amount and types of PAHs formed during the combustion process has been discussed extensively in literature. For instance, studies revealed that using biodiesel in place of conventional diesel significantly reduced the formation of PAHs during combustion (31, 100). Previously, (12) investigated the effect of different fuel types, including diesel, biodiesel, and ethanol, on PAH emissions from a heavy-duty diesel engine. This study affirmed that the fuel type or difference in fuel blend significantly influenced the number and types of PAHs formed during combustion. (76)

investigated how fuel characteristics, including aromatic concentration and boiling point range, affected PAH emissions from a direct injection engine powered by gasoline. Results from this study revealed that fuels with higher aromatic content and a wider boiling point range resulted in higher levels of PAH emissions.

Similarly, temperature and pressure are critical factors that have significant impact in PAH formation and soot nucleation. High-temperature combustion conditions promote the formation of PAHs and their subsequent growth into larger particles. Additionally, high pressure conditions can enhance PAH formation by increasing the residence time of intermediate species in the combustion zone (114). According to a study by (67), higher temperatures and pressures during combustion result in increased PAH formation and soot particle growth. This is due to the increased availability of fuel radicals (Propargyl (C_3H_3) & benzyl ($C_6H_5CH_2$) etc) and intermediate species, which can undergo various reactions to form larger PAHs and ultimately, soot particles.

Other factors, such the presence of trace metals, can also have an impact on how PAHs and soot nucleate. For instance, (49) investigated the impact of trace metals, specifically iron (Fe), on the production of polycyclic aromatic hydrocarbons (PAHs) and soot nucleation using molecular dynamics simulations. Models suggest that Fe atoms accelerate the production of PAHs and the rate of soot nucleation by lowering the temperature at which they fragment. Fe atoms selectively disassemble the C-H bonds and link the PAHs via dehydrogenation at standard flame temperatures. As a result, during the generation of PAH at high temperatures, embedded five- or seven-membered rings are formed. The findings help us understand the physicochemical mechanisms that explain how soot develops during more precise combustion with trace metals.

In summary, nucleation process is a significant phase in soot particle formation within the combustion systems. The formation of initial PAHs from the decomposition of fuel, as well as

their subsequent condensation and growth, are influenced by several factors such as fuel composition, pressure, temperature, and the presence of trace metals. Understanding the fundamental processes that lead to soot nucleation can help engineers create combustion systems that emit fewer dangerous soot particles.

2.3.3.2 *Surface Growth*

Soot particles are the main cause of air pollution, and their proliferation via surface growth is an important process to understand. Surface growth of soot particles occurs through the deposition of additional carbon on their surfaces, and it is a complex process influenced by several factors.

The concentration of hydrocarbons present in the combustion environment largely determines the rate of surface growth. For instance, higher concentrations of hydrocarbons will lead to an increased rate of surface growth. The composition of the combustion environment can also affect the rate of surface growth. In addition to the composition of the combustion environment, temperature and pressure also play a crucial role in surface growth. High-temperature combustion conditions favor the deposition of additional carbon on soot particles, leading to faster surface growth (17). Similarly, high-pressure conditions can enhance surface growth by increasing the residence time of soot particles in the combustion zone (18, 13).

Furthermore, (56) affirmed that the morphology and size of soot particles determine the rate of surface growth. Surface growth influences aggregation kinetics, leading to a time-dependent rivalry between the two phenomena. Surface growth simulations using Monte Carlo discrete element codes have revealed that the number of primary particle coordination is highly dependent on the percentage of particle volume and surface growth rate. As aggregates experience surface expansion, this causes an increase in particle local compacity, reducing both the primary particle and aggregate size distributions.

(16) investigated soot properties in methane and ethylene diffusion flames by examining the soot particle nucleation, surface development, coagulation, agglomeration, and oxidation

processes. The study discovered that the different stages of soot formation in a methane flame were slower than those in an ethylene flame, and that increasing the oxygen content expedited the various stages of soot development. The study also discovered that methane doping can stimulate soot production at various points in the flame, and that under high blending ratio conditions, the fuel's synergistic impact vanishes. As a result, variables like oxygen concentration, fuel type, and blending ratio can affect how quickly soot particles grow on their surfaces, which is affected by the morphology and size of the particles in the combustion system.

The concentration of hydrocarbons, the nature of the combustion environment, temperature, pressure, and the size and morphology of soot particles are only a few of the variables that might affect surface growth. It is possible to create combustion systems that are more effective and less harmful to the environment by understanding these aspects and how they interact.

2.3.3.3 Coagulation

Coagulation is the process where two or more particles come together to form a larger particle.

In the context of soot particles, coagulation occurs when smaller soot particles collide and stick together. The rate of coagulation is determined by factors which include particle size, particle concentration, and turbulence in the combustion system (95). Coagulation is particularly important in high-pressure combustion systems where soot particles are densely packed. Coagulation is a significant process in the growth of soot particles, particularly in high-pressure combustion systems. The coagulation process can occur through a variety of mechanisms, including Brownian diffusion, gravitational settling, and turbulent collisions (115). The rate of coagulation is determined by factors such as particle size, concentration, and turbulence in the combustion system.

Particle size is an important determinant of the rate of coagulation, with larger particles being more likely to collide and stick together. Particle concentration also plays a critical role in

coagulation, as the likelihood of particle collisions increases with increasing particle concentration (96). Turbulence in the combustion system can also influence the rate of coagulation, with high levels of turbulence leading to increased particle collisions and subsequent coagulation.

(8) used SMPS to look at the distribution of nanoparticle sizes in a turbulent non-premixed flame. Prior studies have shown that nanoparticles can coagulate in the sample line and have an uneven particle size distribution when they are not sufficiently diluted. The effects of particle size, particle concentration, and turbulence on the rate of coagulation were investigated by a parametric analysis. (8) discovered that a two-stage dilution procedure can completely remove particle coagulation in the sampling stream. Carbonaceous nanoparticle concentration particle size distribution functions also demonstrate a correlation between turbulence and particle size distribution, which indicates an increase in mean particle diameters with increasing distance from the nozzle along the centreline.

Additionally, research by (101) also reported the effect of coagulation on soot particle growth in different combustion systems. Furthermore, (27) confirmed that coagulation is a critical feature of nascent soot particles, which tend to collide and merge to create larger particles. The resultant substance are regarded as a new primary particle because the initial shape of developing soot particles is lost. Coagulation can have a significant impact on soot particle growth in various combustion systems, and the resulting particle size distribution can affect engine performance and efficiency. Another study by (55) on the transmission of trace metals to form soot particles asserts that the longer collection time means more physical coagulation and larger particle aggregates. This has an impact on the resulting PSD and characterization of the collected soot. In combustion systems, coagulation results in the development of larger particles, affecting the emissions and performance of the engine.

Lastly, the chemical composition of the combustion system can also influence the coagulation process. (44) analyzed the coagulation behavior of soot particles in flames generated from various types of fuels. The study affirmed that the coagulation behavior varied significantly depending on the fuel type, with some fuels exhibiting higher rates of coagulation than others.

2.3.3.4 Oxidation

In addition to the growth mechanisms mentioned earlier, soot particle growth can be influenced by oxidation. Oxidation occurs when soot particles react with oxygen in the combustion system, leading to the development of smaller particles or even their complete oxidation into carbon dioxide. Factors, like pressure, temperature, and the concentration of oxidants influence the process in the combustion system. (26) studied the soot particles' oxidation beneath low-temperature conditions and discovered that the rate of oxidation was dependent on the nitrogen oxide and oxygen's concentration in the combustion system.

Another study affirmed that metal oxide catalysts, specifically Cu-Mn-Ce mixed oxides, improve the oxidation of soot particles. (1) characterized the properties of mixed oxides and results demonstrated that the ternary mixed oxides catalysts exhibited superior soot oxidation performance. The Cu-Mn-Ce catalyst showed exceptional performance in both NO + O₂ and O₂ atmospheres, and the catalysts were also reusable and durable. Therefore, metal oxide catalysts play a critical role in enhancing the oxidation of soot particles for improved combustion system performance and sustainability.

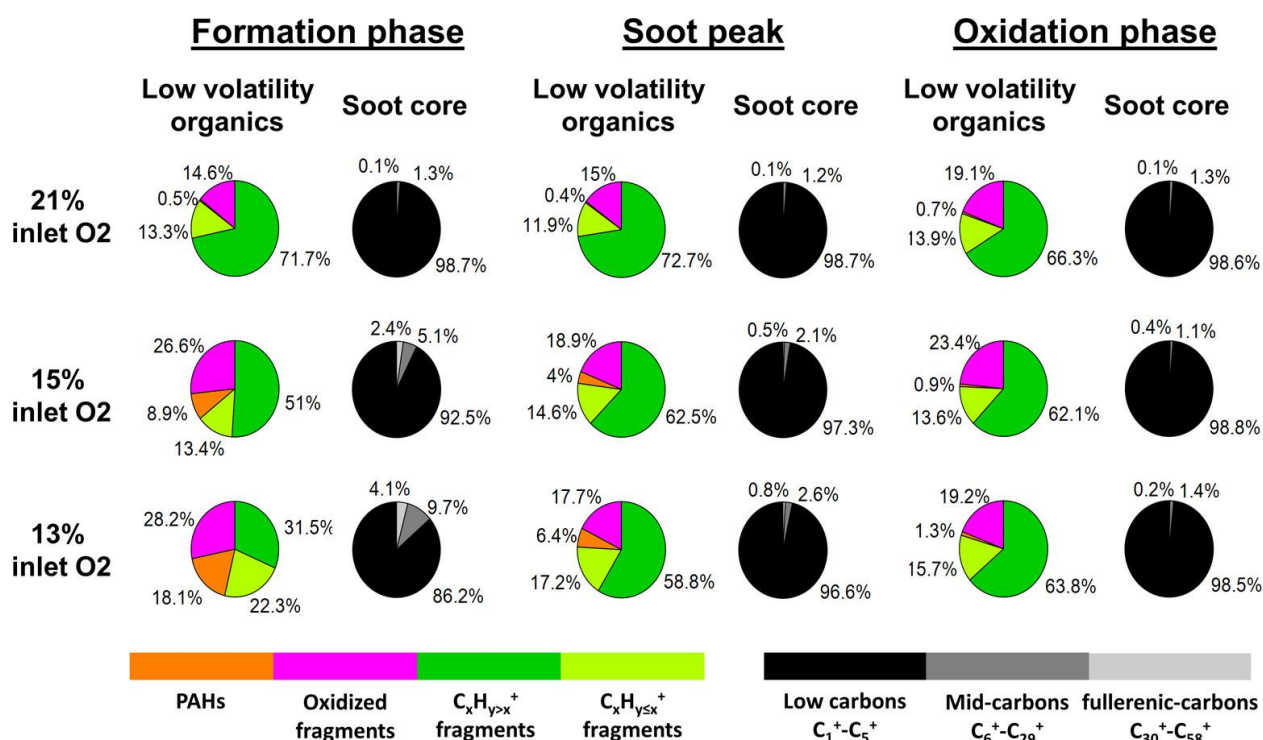


Figure 2.4: Cylinder Soot Formation and Oxidation (48)

2.3.3.5 Fragmentation

Conversely, soot particles can undergo fragmentation in the combustion system when they collide with surfaces or other particles, causing them to break into smaller fragments. The degree of fragmentation is determined by factors such as surface roughness, particle size, and particle concentration. Using molecular dynamics simulations, (50) studied the role of Fe atoms in PAH fragmentation and their impact on PAH development and soot nucleation. The research delved into how the Fe collision orientation, energy, and equilibrium temperature of PAH molecules influence PAH fragmentation. The presence of Fe atoms was found to significantly increase the PAH development and soot nucleation rate by reducing the PAH fragmentation temperature. Fe atoms were also observed to break C-H and C-C bonds, connecting PAHs through dehydrogenation. Overall, the research provides valuable insights on the importance of fragmentation in soot formation during combustion with trace metals (50).

In conclusion, the growth or development of soot particles in combustion systems occurs through several mechanisms, including nucleation, surface growth, and coagulation.

Understanding the mechanism is essential for the development of effective strategies for reducing soot emissions from combustion systems. The rate and extent of soot particle growth are affected by several factors which include fuel composition, pressure, temperature, and turbulence, which need to be considered when designing combustion systems.

2.4 Effect of Fuel Type, Combustion Conditions, and other Factors on Soot Particle Formation and Growth

Several studies have focused on investigating the effects of fuel type, combustion conditions, and other factors on the formation and growth of soot particles during combustion. The chemical composition of the fuel is a critical factor that influences the quantity and characteristics of the soot particles produced. Aromatic hydrocarbons, for instance, are known to produce more soot than aliphatic hydrocarbons due to their higher carbon-to-hydrogen ratio (C/H) (26).

(88) evaluated the impact of various fuels on soot morphology, oxidative reactivity and nanostructure. The research affirmed that the molecular weight and other fuel characteristics, such as aromaticity, had a substantial impact on the soot characteristics, with increased aromaticity leading in the creation of larger, more stable soot particles. Therefore, in comparison to the modes using diesel/ gasoline and diesel/methanol, (39) found that the usage of toluene/diesel fuel blend produced the maximum number of soot particles. Specifically, it was discovered that there was 54% more soot in the diesel/toluene mode than in the diesel/gasoline mode. The study also evaluated the structure of the soot particles and their distributions by size and particle mass by size.

(84) examined how fuel properties affected the size and morphology of soot particles in a turbulent diffusion flame. The research demonstrates that soot particles were larger and more complex when formed by fuels with higher aromatic concentration and molecular weight. In addition to fuel properties, the formation and growth of soot particles were dependent on combustion circumstances like temperature and pressure.

(90) investigated the effects of combustion pressure on soot particle characteristics in a laminar premixed flame. The researchers found that increasing combustion pressure led to an increase in soot particle size and concentration. Similar research was conducted by (60).

In addition to fuel type, combustion conditions such as pressure, temperature, residence time, and oxygen concentration also affect soot particle formation and growth. Increasing the combustion temperature promotes soot particle formation by increasing the rates of chemical reactions that lead to soot formation (46). However, at high temperatures, soot particles can also undergo oxidation and fragmentation, leading to smaller particle sizes. Higher pressures and longer residence times tend to promote soot particle growth by allowing more time for the soot particles to coagulate and surface growth to occur (18). Turbulence, on the other hand, promotes soot particle formation by enhancing mixing and transport of reactants and products, leading to increased rates of chemical reactions that produce soot precursors.

Studies in the past decade demonstrate the impact of various species present in the combustion environment on soot particle formation and growth. (90) stated that the addition of carbon dioxide, hydrogen, and water vapor have an impact on the development and growth of soot particles in combustion. Hydrogen has a chemical effect that primarily affects the soot nucleation process, whereas carbon dioxide indirectly affects soot production via the $\text{CO} + \text{OH} \leftrightarrow \text{CO}_2 + \text{H}$ reaction. Water vapor mostly raises OH concentrations while weakening the soot nucleation process.

Sulfur compounds are another species that has been demonstrated to influence soot particle production and growth. According to (105), high fuel sulfur content (FSC) increases soot particle concentrations of sulfur functional groups (SFGs), as well as primary particle size and volatile organic fraction (VOF) content. Some SFGs, such as -SH and C-S, can boost soot oxidation reactivity while decreasing oxidation activation energy. Metal-sulfates, such as CaSO_4 , produced by the reaction of SO_2 with metal components in fuel or lubricant oils, can

help improve soot oxidation. Overall, the findings indicate that sulfur plays a significant role in the physicochemical properties and oxidation behavior of soot particles produced by FSC fuels.

Similarly, metals like iron and copper impact the development and generation of soot particles. The introduction of an iron-based fuel borne catalyst (Fe-FBC) in diesel fuel significantly reduces area occupation ratio and soot concentration in cylinder, and decreases soot, HC, CO, HCHO, CH₃CHO and PAHs emissions (44). Fe-FBC addition also weakens the polymerization degree between particles, resulting in a more sparse and loose arrangement of particles, and significantly decreases the temperature, activation energy, and oxidation properties of soot particles.

In addition, the presence of Fe-FBC addition can drastically lower the kind and concentration of PAHs and high carbon atom number compounds in exhaust particles (44). Likewise, (64) stated that helicoidally shaped copper duct in a diesel engine showed a reduction in soot emissions of up to 28% compared to the baseline, without any significant change in combustion delay. The increase in copper content in the fuel resulted in an oxidizing effect that reduced soot formation. However, when a non-metallic Teflon duct was used, no significant effect on combustion and emission characteristics was observed.

Overall, previous studies have shown that multiple factors influence soot particle formation and growth in combustion systems, and the interactions between these factors can be complex. Understanding these effects is crucial for optimizing combustion processes to minimize soot particle emissions and improve combustion efficiency.

2.5 Experimental Techniques for Measuring Soot Particle Size Distribution

Accurate and reliable monitoring of soot particle size and concentration is necessary for studying the generation and development of soot in micro-scale combustion systems. Various experimental approaches have been developed to determine the distribution of soot particles. Each technique has its advantages and limitations, which must be carefully considered for

optimal experimental design and interpretation of results. Previous studies have successfully utilized these techniques to investigate soot particle distribution in micro-scale combustors, providing valuable insights into the complex nature of soot formation in these systems (40; 36).

2.5.1 Experimental Techniques for Soot Particle Size and Concentration

Measuring the size and concentration of soot particles is crucial in understanding their formation and growth during combustion processes. Various experimental techniques such as microscopy, laser-induced incandescence, and thermophoretic sampling have been developed to measure soot particle size and concentration, each with its advantages and limitations.

Table 1: Description, Advantages and Limitations of Experimental Techniques

| Technique | Description | Advantages | Limitations |
|-----------------------------------|---|--|---|
| Microscopy | Provides direct visualization of soot particles, allowing for precise determination of particle size and morphology (40). | Can observe internal structure and composition of soot particles (40). | Time-consuming sample preparation and image analysis. Only provides information on a limited number of particles at a time. May not be suitable for in situ measurements of soot particle size and concentration in real-time (53). |
| Laser-induced incandescence (LII) | Non-intrusive technique that uses a laser beam to heat soot particles, | Provides high spatial and temporal resolution. Relatively | Sensitive to the optical properties of the soot particles. Limited to |

| | | | |
|-------------------------|---|--|--|
| | causing them to emit light in the infrared region, which is then detected and analyzed to determine particle size and concentration (7). | simple and cost-effective compared to other methods (11). | measuring particles in a certain size range, typically between 10 and 500 nm (6). |
| Thermophoretic Sampling | Uses a probe to collect particles that have been thermophoretically deposited on a surface. The collected particles are then analyzed using techniques such as microscopy or transmission electron microscopy (TEM). (36) | Can measure particle size distribution and concentration in situ, without interfering with the combustion process. Allows for the collection of particles in a controlled manner (84). | Potential for particle loss during the sampling process. Potential for sampling bias (10). |
| SMPS | tool for determining the size distribution of submicron particles in the environment. The SMPS separates particles based on their electrical mobility, which is determined by their size and charge (92) | It provides real time measurement of particles. The uncertainty is less than 10%. It also has a resolution measuring 2nm to 100nm (62) | Limited information on particle composition: SMPS provides information on particle size distribution, but not on the chemical composition or morphology of the particles |

Microscopy is an experimental technique that is broadly used to determine soot particle size and concentration in different types of combustion systems. This technique involves the use of specialized microscopes to observe and measure the morphology and size distribution of soot particles (63). Microscopy techniques have several advantages, including the ability to provide high-resolution images of individual particles and to differentiate between different types of particles based on their morphology (40). However, they also have some limitations, such as the inability to provide quantitative information on particle concentration and size distribution (53).

Microscopy has been used in several investigations to analyze the size and shape of soot particles in various combustion systems. (28) studied the size and morphology of soot particles in a Jet-Stirred Reactor (JSR) by collecting released particles on quartz fiber filters and studying them with HRTEM and Raman methods. The shape and nanostructure properties of the soot particles were determined using HRTEM images and Raman spectra of filter-laden soot samples. The researchers discovered that different combustion variables, such as combustion pressures, fuel flow rates, and input air temperatures, altered the size and shape of the soot particles. (15) also adopted HRTEM to examine the size and morphology of soot particles generated by internal combustion engines. This approach enables extensive examination of the physical characteristics and nanostructure of engine soot agglomerates, revealing critical information for understanding the soot generation process, particle behavior in after-treatment systems, and nano-particle health implications.

Furthermore, in a co-flow diffusion fire (37) employed TEM to investigate the nanostructure and primary particle diameter of soot particles. For primary particle sizes, the TEM results matched with time-resolved laser-induced incandescence. The researchers also discovered that the fractal dimension of soot aggregates reduced with time. Overall, TEM gave helpful information on soot particle size and shape in various combustion systems. (101) used Thermophoretic Sampling, TEM, and fractal-based methods to investigate the size and

structure of soot particles in anisole/n-heptane flames. Anisole influenced the soot generation process, resulting in bigger primary particle sizes. The study thoroughly examined primary particle diameter distributions, aggregate sizes, and fractal dimensions.

Microscope methods have also been utilized to analyze the development and growth of soot particles in micro flow tube reactors. For instance, (80), applied TEM to evaluate the soot particle size and shape in a MFTR under varied operating settings. They discovered that the reactor temperature and residence time had a significant impact on the size and shape of the soot particles. (101) investigated the shape and size distribution of soot particles in a MFTR powered by diesel and n-heptane blends using SEM. The studies revealed that soot particles were largely agglomerates of primary particles, and that the particle size distribution was substantially controlled by the fuel mix.

Laser-induced incandescence (LII) is an experimental technique used in determining the size and concentration of soot particles in a combustion environment. LII is a non-intrusive technique that involves illuminating soot particles with a laser pulse, causing the particles to heat up and emit incandescent light, which is then detected by a photodetector (63). The size of the soot particles can be determined from the time taken for the particles to reach their maximum temperature and the rate at which they cool down, while the concentration of soot particles can be estimated from the intensity of the emitted light (45).

One of the advantages of LII is that it provides high spatial and temporal resolution, allowing for the measurement of soot particle size and concentration in real-time with good accuracy (116). Additionally, LII can be used in harsh combustion environments, such as gas turbine engines and diesel engines (117). However, the accuracy of LII measurements can be affected by factors such as laser energy, particle composition, and laser scattering (63).

Several studies have used LII to measure soot particle size and concentration in various combustion environments. For example, (116) used LII to study the effects of pressure on soot

particle formation in a laminar premixed flame. They found that increasing the pressure led to smaller soot particle sizes and higher particle concentrations. (45) used LII to investigate the effects of different fuel types on soot particle formation in a diffusion flame. The study revealed that the fuel type had a significant influence on soot particle size and concentration. (117) used LII to study the effect of swirl on soot particle formation in a premixed swirl burner. They found that increasing swirl led to smaller soot particle sizes and higher particle concentrations.

Thermophoretic sampling is an experimental technique used to measure soot particle size and concentration. This technique is based on the principle of thermal precipitation, which occurs when soot particles move toward a colder surface due to the temperature gradient created by a hot gas stream. The soot particles deposit onto the colder surface, which can be analyzed to determine the size and concentration of the particles. One advantage of this technique is that it allows for continuous measurement of soot particles in real-time, making it suitable for use in high-temperature environments (117).

In earlier research, soot particle size and concentration in diverse combustion systems were measured using thermophoretic sampling. For instance, (106) used it to investigate soot particle emissions from a diesel engine, while (117) utilized it to research soot generation in a laminar premixed flame. In a different investigation by (118), soot particle concentration and size distribution in a gas turbine combustor were measured using thermophoretic sampling.

Despite its advantages, thermophoretic sampling has some limitations. For instance, the technique is sensitive to changes in gas temperature, which affects the soot particles deposition onto the sampling surface. Similarly, the sampling surface can become contaminated over time, which affects the accuracy of the measurements. Nonetheless, thermophoretic sampling is a useful method for determining the size and quantity of soot particles in a variety of combustion systems.

2.5.2 SMPS Technique for Measuring Soot Particle Size

The section introduces three main types of computational techniques namely Scanning Mobility Particle Sizer (SMPS), Differential Mobility Analyzer (DMA) and Electrical Low-Pressure Impactor (ELPI). Furthermore, a comparative analysis is carried out to determine the most suitable method for studying the size distribution of a micro flow tube reactor.

The Scanning Mobility Particle Sizer (SMPS) is a popular tool for determining the size distribution of submicron particles in the environment. The SMPS separates particles based on their electrical mobility, which is determined by their size and charge. The instrument has been used in a variety of applications, including atmospheric monitoring, combustion research, and nanotechnology. According to a study by (92), the SMPS was used to measure the size distribution of aerosol particles during haze events in China. The study found that the PSD changed during the haze events, with an increase in the number of particles in the submicron size range. The SMPS was able to measure the changes in particle size distribution with high accuracy and precision.

Another study by (74) investigates the soot PSD in premixed turbulent ethylene-air flames using the SMPS. To analyze the evolution of particle size distributions via the turbulent flame brush, the SMPS is employed to provide data that is spatially resolved along the stagnation point streamline. The application of SMPS in this study allows for a detailed characterization of PSD in the premixed turbulent ethylene-air flames crossing the soot inception limit. Conversely, (41), determined the size distribution of atmospheric particles using the SMPS. An analytical method to predict PSD under changing concentration is introduced in this study. The approach is validated by conducting tests with exponentially decaying particle concentration. The research provides insights on the significance of precise SMPS measurements in highly changing particle concentrations over time.

The Differential Mobility Analyzer (DMA) and Electrical Low-Pressure Impactor (ELPI) are two instruments used to determine the PSD of the aerosol. The DMA is commonly used

instrument for determining the aerosol's PSD. It separates particles based on their electrical mobility, which is related to their charge and size. (3) analyzed the solid nucleation mode particles generated by gasoline and diesel direct injection engines using an Advanced Half Mini DMA (HM-DMA). At up to 200°C, the device can categorize aerosol particles with mobility sizes ranging from 5 to 30 nm with high resolution and quick spectrum capture. The accuracy of the Advanced HM-DMA hot operation mode is examined and compared to State-of-the-Art instruments, and it provides a reliable and simplified method for measuring solid nucleation-mode particles.

The ELPI is a device that uses multiple stages of impactors to measure the size distribution of aerosol particles based on their aerodynamic diameter. The ELPI (Electrical Low Pressure Impactor) was employed in a study by (19) as a measurement device to identify particles based on their inertial behavior and size range. The study used several collection substrates and impactor plates to see how particle loss and particle bounce affected the ELPI+ findings. The aim of the research was to evaluate the impact of these mechanisms on the measurement of particulate matter emissions.

Table 2: Comparative Analysis of the Three Sampling Techniques for Measuring Soot Particle Size

| Parameter | SMPS | DMA | ELPI |
|------------------|---|--|---|
| Principle | Measures particle size based on electrical mobility | Separates particles based on electrical mobility | Separates particles based on aerodynamic diameter |

| | | | |
|---------------------|------------------------|-------------------------|--------------------------|
| Particle Size Range | 1 nm - 1 μm | 1 nm - 10 μm | 30 nm - 10 μm |
| Number of Size Bins | Up to 600 | Up to 128 | Up to 12 |
| Sample Flow Rate | 0.1 - 2.0 L/min | 0.1 - 10 L/min | 2.3 L/min |
| Accuracy | High | High | Medium |
| Precision | High | High | High |
| Sensitivity | High | Medium | Medium |
| Complexity | High | Medium | Low |
| Cost | High | Medium | Low |
| Resolution | High | Medium | Low |

The comparative analysis shows that SMPS, DMA, and ELPI have different ranges of particle sizes they can measure and different sample flow rates. SMPS has the highest sensitivity and resolution and is the most complex and expensive of the three instruments. DMA has a higher resolution than ELPI, but a lower number of size bins and a medium level of complexity. ELPI has the lowest complexity and cost, but also the lowest resolution and sensitivity. All three instruments have high precision, but the accuracy varies depending on the instrument and the conditions of the measurement. The choice of instrument depends on the specific application and the required parameters, such as particle size range, resolution, and sensitivity. In summary, the SMPS is a widely used instrument for measuring the size distribution of submicron particles in various applications. The ability of SMPS to measure changes accurately and precisely in particle size distribution makes it a valuable tool in atmospheric monitoring, combustion research, and nanotechnology research.

2.6 Advantages and Limitations of Experimental and Modeling Method

Experimental approaches have the advantage of directly measuring real-world phenomena, providing empirical data that can be used to validate models and simulations. Experimental techniques such as microscopy, LII, and thermophoretic sampling offer high spatial and temporal resolution, allowing for the measurement of soot particle size and concentration under various combustion conditions. They can also provide insights into the physical and chemical processes that occur during combustion. However, experimental techniques can be expensive, time-consuming, and require specialized equipment and expertise. They can also be limited by issues such as interference from other particles and limitations in the sensitivity and accuracy of the measurement techniques.

Table 3: Experimental Method

| s/n | Advantages | Limitations |
|-----|---|--|
| 1 | Provides direct measurement of soot particle size and concentration | Limited spatial resolution and inability to capture rapid temporal variations in particle distribution |
| 2 | Multiple techniques available, each with its own strengths and weaknesses | Limited sensitivity to smaller particles |
| 3 | Non-intrusive, minimally disruptive to combustion system | Limited ability to distinguish between soot particles and other carbonaceous species |
| 4 | Can be used in situ or ex situ | Sampling methods may introduce artifacts or biases |

| | | |
|---|--|--|
| 5 | Can provide information on morphology and chemical composition of soot particles | May require significant time and cost to set up and conduct experiments. |
| 6 | Can be used to validate modeling predictions | Requires specialized equipment and expertise |

On the other hand, modeling approaches offer the advantage of being cost-effective, flexible, and easily modifiable. They can be used to predict the behavior of complex systems under various conditions and can provide insights into the underlying physical and chemical processes that occur during combustion. Modeling approaches such as sectional modeling can also provide detailed information about the size and distribution of soot particles. However, modeling approaches are only as good as the accuracy of the underlying assumptions and input parameters used in the model. They also require validation against experimental data to ensure their accuracy and reliability.

Table 4: Modeling Method

| s/n | Advantages | Limitation |
|-----|---|---|
| 1 | Can provide detailed spatial and temporal information on soot particle distribution | Model predictions may not accurately reflect real-world combustion conditions or physical processes |
| 2 | Can be used to study a wide range of operating conditions and geometries | Model predictions are dependent on assumptions and input parameters |
| 3 | Can identify key processes controlling soot particle formation and growth | Models may be computationally expensive and require significant computational resources |

| | | |
|---|--|---|
| 4 | Can be used to optimize combustion processes and design more efficient and cleaner systems | Models may not accurately capture the full complexity of combustion chemistry and physics |
| 5 | Can provide insights into the underlying mechanisms of soot particle formation and growth | Requires validation against experimental data to ensure accuracy |
| 6 | Can predict soot particle size and concentration under conditions that are difficult to measure experimentally | Models may require simplifying assumptions that can affect accuracy |
| 7 | Can be used to explore new combustion concepts and technologies | Requires specialized software and expertise |

Overall, both experimental and modeling methods have benefits and drawbacks, and it is sometimes required to combine both methods to properly comprehend the behavior of soot particles in combustion systems. Combining experimental and sectional methods can result in a determination of the soot particle size distribution function that is both more thorough and precise. While sectional techniques offer insights into the mechanisms governing particle creation and development, experimental methods like TEM and scanning mobility particle sizing (SMPS) directly measure the size distribution of the particles. Combining these methods makes it feasible to test and enhance sectional models, which can help us comprehend the underlying physical and chemical mechanisms that regulate the creation and development of soot particles in combustion systems.

Previous studies demonstrate the application of both approaches to achieve better results. To study the soot particle generation and development in a laminar ethylene-air diffusion flame, (60) utilized experimental and sectional methodologies. The work employed sectional

approaches to describe the particle creation and growth processes using TEM and SMPS to assess the particle size distribution. The findings demonstrated that the sectional method could reproduce the experimental data and offering insights into the mechanisms behind the development and production of soot particles, including the significance of particle-particle interactions and the function of polycyclic aromatic hydrocarbons (PAHs).

Similar methods were employed in different research by (120) to look at the development and production of soot particles in a laminar premixed ethylene flame. The study employed sectional approaches to describe the particle generation and growth processes and SMPS to assess the particle size distribution. The outcomes demonstrated that the sectional technique could replicate the experimental data and offer insights into how temperature and fuel concentration affected the production and development of soot particles.

In conclusion, the combination of experimental and sectional methods, like SMPS, can offer a more thorough and accurate measurement of the soot particle size distribution function and can result in a better comprehension of the underlying physical and chemical processes that regulate soot particle formation and growth in combustion systems.

2.7 Identification of Gaps in Literature and Potential Areas for Future Research

Despite the significant progress in the research on soot particle distribution in micro flow tube reactors using experimental and modeling approaches, several gaps and inconsistencies in the literature exist. These gaps and inconsistencies indicate potential areas for future research, which can improve our understanding of soot formation and oxidation processes in these reactors. One of the gaps in the literature is the lack of systematic and comprehensive comparisons between experimental and modeling results. Although some studies have compared the two sets of results, most of them have focused on qualitative comparisons, without investigating the quantitative agreement between the experimental and modeling data. Furthermore, some studies have used simplified models or assumptions, which may not

accurately represent the complex processes in MFTR. Therefore, there is a need for more rigorous and detailed comparisons between experimental and modeling results, using more accurate and realistic models.

Another gap in the literature is the limited knowledge on the effects of reactor operating conditions on soot particle distribution. While some studies have investigated the effects of parameters such as fuel type, equivalence ratio, and residence time, others have focused on the effects of inlet boundary conditions or reactor geometry. However, there is a need for more systematic and comprehensive studies that investigate the effects of multiple operating parameters on soot particle distribution in MFTR.

Furthermore, most of the studies on soot particle distribution in MFTR have focused on the steady-state behavior of the system, without considering the transient behavior during startup or shutdown. Transient behavior is important for understanding the dynamic response of the system to changes in operating conditions, and it can also affect the soot particle distribution. Therefore, future research should investigate the transient behavior of MFTR and its effects on soot particle distribution.

Another potential area for future research is the development of more accurate and realistic models for soot particle formation and oxidation in MFTR. While some studies have used detailed kinetic mechanisms and reaction pathways, others have used simplified models or empirical correlations. Therefore, there is a need for more accurate and realistic models that can capture the complex physicochemical processes involved in soot formation and oxidation in MFTR.

The physical and chemical characteristics of soot particles in MFTR need to be studied further in experimental research, which is the final point. While some studies have examined the size and quantity of soot particles, few have investigated their morphology or chemical makeup. Furthermore, little is known about how the characteristics of soot particles affect the operation

of reactors and emissions. Future studies should thus investigate the physicochemical makeup of soot particles in MFTR and how that affects the operation and emissions of the reactor.

In conclusion, the existing literature on soot particle distribution in MFTR using experimental and modeling approaches has made significant progress in the past decade. However, several gaps and inconsistencies in the literature indicate potential areas for future research, which can improve our understanding of soot formation and oxidation processes in these reactors.

3. METHODOLOGY

3.1 Experimental setup

In this work, two distinct experimental configurations are used, one for the atmospheric pressure pyrolysis/oxidation case and the other for high pressure pyrolysis/oxidation experiments. For the high-pressure experiments, a microflow straight tube reactor with a converging-diverging section was designed.

Both experiments constituted the same flow configuration setup, except for the pressure vessel used for the high-pressure case. Due to the wide range of acceptance, the measurement tool employed for this study was the nano Scanning Mobility Particle Sizer (n-SMPS). The SMPS which is a TSI model consists of a nano-Differential mobility analyzer (n-DMA 3085), a classifier (model 3080) and the nano-Condensation Particle Counter (n-CPC model 3788). This subcomponent makes the machine a choice tool especially for particle measurement. For this experiment, in order to achieve the best resolution, the sheath flow rate was set to 6 lpm while the inlet flow rate was set to 1.5 lpm with a particle size range of 3nm to 105 nm.

3.1.1 Set up for Micro flow tube reactor (MFTR)

The experimental setup consists of 7 modular heaters and each of them are controlled by a set of K-type thermocouples, PID's (proportional integral derivative), and SSR's (solid state relay) (see Fig. 3.1). The heating elements can reach a maximum temperature of 1323 K. The reactor is customized made with 4 mm ID and 62.5 cm long quartz tube, with two opposed side arms

located at 27.5 cm from the inlet to introduce a mixture of oxygen and nitrogen. The ID of side arms are 1 mm so that it can rapidly mix with the main flow allowing the assumption of step change in composition at the junction with the main flow.

For the different jet fuels, the fuels were pre-vaporized using an ultrasonic atomizer and mixed with heated N_2 carrier gas. The flow rate of fuel was controlled using a syringe pump, while the flow rates of gases (N_2 and O_2) were controlled using Sierra 100 series mass flow controllers. The fuel/ N_2 / O_2 delivery lines were maintained at a temperature of about 500 K, well below the pyrolysis temperature of the fuel at residence times in the supply lines (see Fig. 3.1).

Figure 3.1: Schematic of the experimental setup showing key features and components.

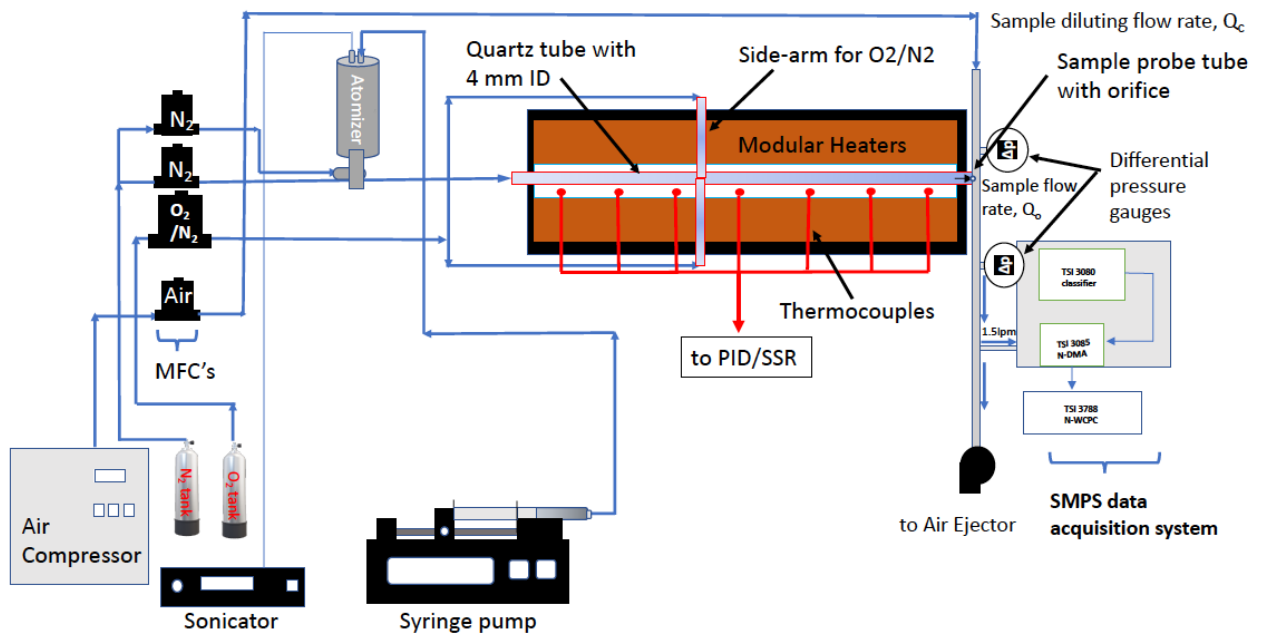




Figure 3.2: Actual image of the experimental setup.

The SMPS system was mounted on a portable equipment rack (see Fig. 3.2) with an Inconel sampling probe tube having a $250\mu\text{m}$ orifice which can be readily centered at the exit of the tube reactor. The sampling probe is supplied with filtered diluting air with a dilution ratio of 2000-2500 to eliminate any particle loss to tube walls or particle-particle coagulation. The pressure of the sampling probe is maintained at a slightly negative pressure (25-250 Pa) by continuously monitoring the pressure via two gauges connected on either side of the orifice (see Fig. 3.1). This setup is similar to that used by Wang and co-workers (2003). The mass flow rate through the orifice was calibrated via Sierra 100 series mass flow controllers (1% uncertainty at full scale) as well as the mass flow rate of the diluting air.



Figure 3.3: Image of the portable SMPS setup with 250 μ m probe orifice mounted on an equipment rack.

3.1.2 New high-pressure chamber/reactor

For high-pressure investigations, a new pressure chamber was designed and fabricated (Fig. 3.3). The new chamber consists of 16" ID and 30" length working space. This allowed much easier insertion of the heating elements and the quartz tube with side arms into the pressure chamber. The chamber was hydro tested to a pressure of 40 atm with a target maximum operating pressure of 20 atm.

After completing the atmospheric pressure tests with Jet A, Jet C1 and Jet, we proceeded to move the modular heaters into the high-pressure chamber shown in Fig. 3.3, followed by soot PSD data acquisition as a function of pressure.



Figure 3.4: New high-pressure enclosure with 16” ID and 30” length, with provision for sliding in and out the modular heaters mounted on a V-shape trough.

3.2 Scanning Mobility Particle Sizer

SMPS is a high-resolution nanoparticle sizer which allows real time online sizing of soot particles obtained from different flow conditions. The nano-SMPS used in this work is a TSI model consisting of a Classifier, nano-Differential Mobility Analyzer and a nano-Condensation Particle Counter. The aerosol particles first enter the Classifier through an Impactor. Inside the Classifier the aerosol particles are charged. These charged particles are selected using electrical classification (electrical mobility) inside n-DMA. The selected particles are counted in the n-CPC.

A small sample of flow rate 1.5 lpm is fed to the n-SMPS through an Inertial Impactor (93) which removes particles above a known particle size by accelerating the flow through a 0.071 cm nozzle directed at a plate (Fig. 3.3). The aerodynamic particle size (109) at which the particles are separated is called the cut-point diameter (D_{50}) and is given by:

$$D_{50} = \sqrt{\frac{9\pi St \mu W^3}{4\rho_s C Q}} \quad (3.1)$$

Where, D_{50} is the particle cut-point diameter (cm, 50% cut efficiency), St is the Stokes number (0.23), ρ_s is the particle density (g/cm^3), Q is the volumetric flow rate (cm^3/s), D_p is the particle diameter (cm), μ is gas viscosity (dynes/cm^2), W is the nozzle diameter (cm), and C is the Cunningham Slip Correction factor given by,

$$C = 1 + Kn[\alpha + \beta \exp(-\frac{\gamma}{Kn})] \quad (3.2)$$

Here, $\alpha = 1:142$; $\beta = 0:558$; $\gamma = 0:999$, Kn is the Knudsen number: $Kn = 2\lambda/D_p$ and λ is the gas mean free path

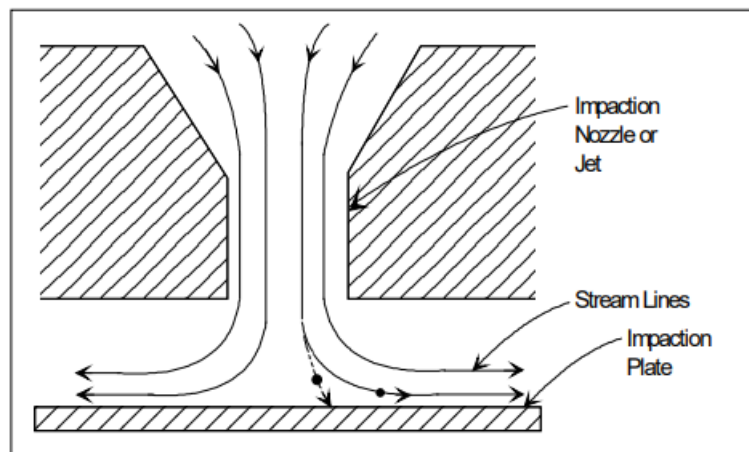


Figure 3.5: Cross-Sectional View of an Inertial Impactor (93)

In the Electrostatic Classifier, the particles enter a Kr-85 Bipolar Charger (or neutralizer) which exposes the aerosol particles to high concentrations of bipolar ions. The particles and ions undergo frequent collisions due to the random thermal motion of the ions. The particles quickly reach a state of charge equilibrium, in which the particles carry a known bipolar charge distribution. The charged soot particles pass from the neutralizer into the main portion of the Differential Mobility Analyzer (DMA), shown in Fig. 3.6. The DMA contains two concentric

metal cylinders. The polydisperse particles and sheath air are introduced at the top of the Classifier and flow down the annular space between the cylinders. The particle flow surrounds the inner core of sheath air, and both flows pass down the annulus with no mixing of the two laminar streams. The inner cylinder, the collector rod, is maintained at a controlled negative voltage, while the outer cylinder is electrically grounded. This creates an electric field between the two cylinders. The electric field causes positively charged particles to be attracted through the sheath air to the negatively charged collector rod. Particles are precipitated along the length of the collector rod.

The location of the precipitating particles depends on the Classifier flow rates, the Classifier geometry and the particle electrical mobility (Z) given by Eq. 3.3 [110, 111]. Particles with a high electrical mobility are precipitated along the upper portion of the rod; particles with a low electrical mobility are collected on the lower portion of the rod. Particles within a narrow range of electrical mobility exit with the monodisperse air flow through a small slit located at the bottom of the collector rod. These particles are transferred to a particle sensor to determine the particle concentration. The remaining particles are removed from the Classifier via the excess air flow.

$$Z = \frac{neC}{3\pi\mu D_p^{mobility}} \quad (3.3)$$

where; n is the number of elementary charges on the particle, e is the elementary charge (1.6×10^{19} Coulomb) and $D_p^{mobility}$ is the diameter of the particle measured by SMPS (cm).

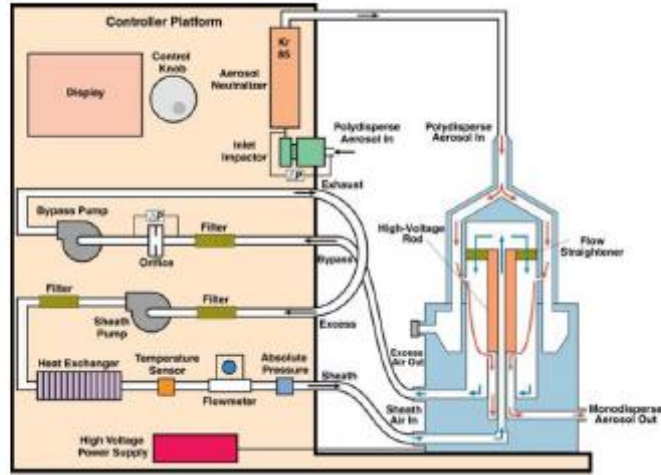


Figure 3.6: Flow schematic for the Electrostatic Classifier with nano-DMA in dual blower mode [62]

The mono-disperse particles exiting the DMA enter the nano-Water Condensation Particle Counter (n-WCPC) where the particles are enlarged by a condensing vapor to form easily detectable droplets. The vapor surrounding the particles reaches a certain degree of supersaturation and begins to condense onto the particles. The degree of supersaturation is measured as the supersaturation ratio (P/P_s), which is defined as the actual vapor partial-pressure divided by the saturation vapor pressure for a given temperature.

For a given saturation ratio, the vapor can condense onto particles only if they are big enough. The minimum particle size capable of acting as a condensation nucleus is called the Kelvin diameter [47, 109]

$$\frac{P}{P_s} = \exp\left(\frac{4\gamma M}{\rho_c R T d_{kelvin}}\right) \quad (3.4)$$

Where, γ is the surface tension of the condensing fluid, M is the molecular weight of the condensing fluid, ρ_c is the density of the condensing fluid, T is the absolute temperature, d_{kelvin} is the Kelvin diameter.

The sensor inside the n-WCPC contains a conditioner, a growth tube, and an optical detector (Fig. 3.7). The sample flow is cooled with a thermo-electric device in the conditioner. The

vapor passes into the growth tube where it becomes supersaturated and condenses onto the particles to form large droplets. The large droplets are detected by the optical detector which uses a laser diode. The current model of n-WCPC counts single particles with continuous, live-time coincidence correction up to 4×10^5 particles/cm³.

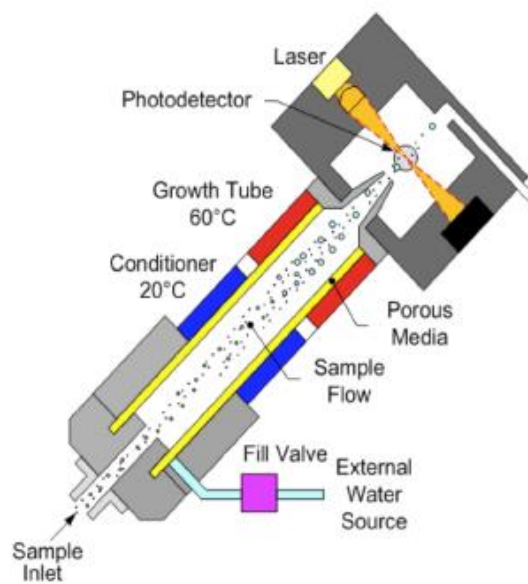


Figure 3.7: Flow schematic for the nano-CPC [62]

In the present study the setting of SMPS was set to allow an inlet sample flow rate of 1.5 lpm and sheath-flow rate of 6 lpm in a dual blower mode which helped in reducing transport time and, therefore, diffusive particle losses. The n-CPC in these settings has lower size limit of 3nm. Typically, a particle size spectrum was obtained from a 120 s up-scan and a 15 s down-scan.

3.2.1 Mobility Diameter

Mobility diameter is the particle diameter measured by SMPS which is based on the electrical mobility in the zero-strength limit (108). The technique used in SMPS to calculate electrical mobility employs empirical Stokes-Cunningham formula given by Eq. 3.3 (47, 109).

In the studies conducted by Li et al. (107, 112) and others (111), it was found that Eq. 3.3 is limited in its accuracy for nano-sized particles. It was proposed (112) that for an ideal gas with $Kn \ll 1$, the particle mobility be modeled as

$$Z = \frac{3}{2} \sqrt{\frac{kT}{2\pi m_r} \frac{pne}{D_p^2 \Omega_{avg}^{(1,1)*}}} \quad (3.5)$$

where, k is the Boltzmann constant, T is the temperature, m_r is the reduced mass, p is pressure, D_p is the proposed true particle diameter and $\Omega_{avg}^{(1,1)*}$ is the average reduced collision integral given by [112]. The relationship between the mobility diameter (D_p^{mobility}) and the true diameter (D_p) is obtained from equating Eq. 3.3 and 3.5 and is plotted in Fig. 3.8. The particle diameter measured by SMPS is corrected based on this fit (Fig. 3.8) in all the measured results presented in this work.

3.3 Calibration of Orifice Flow Rate

As the hot flame gases are drawn into the probe, they are diluted by a carrier gas (cold nitrogen in this case). The dilution ratio between the incoming hot gases and the carrier nitrogen gas is obtained by calculating the volumetric flow rate of flame gases.

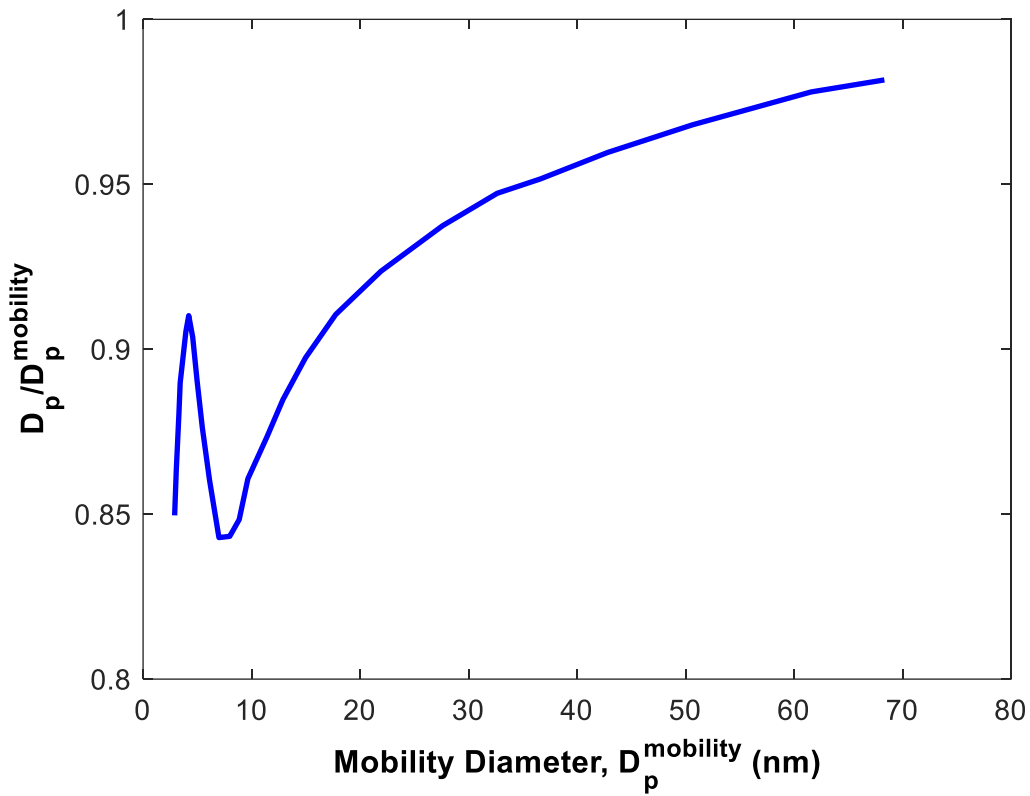


Figure 3.8: Relation between particle diameter and the mobility diameter

through the orifice. The volumetric flow rate of carrier gas nitrogen (Q_c) for experiments was kept constant at 42 lpm. The flow rate through the orifice is calibrated by plugging one end of the probe and connecting its other end to a pump through a flow meter in purge mode. A pressure transducer is connected upstream of the orifice. Atmospheric air at different temperatures is used to calibrate the probe orifice. The observed volumetric flow rate versus differential pressure across orifice for a probe with 250 μ m orifice is plotted in Fig. 3.9.

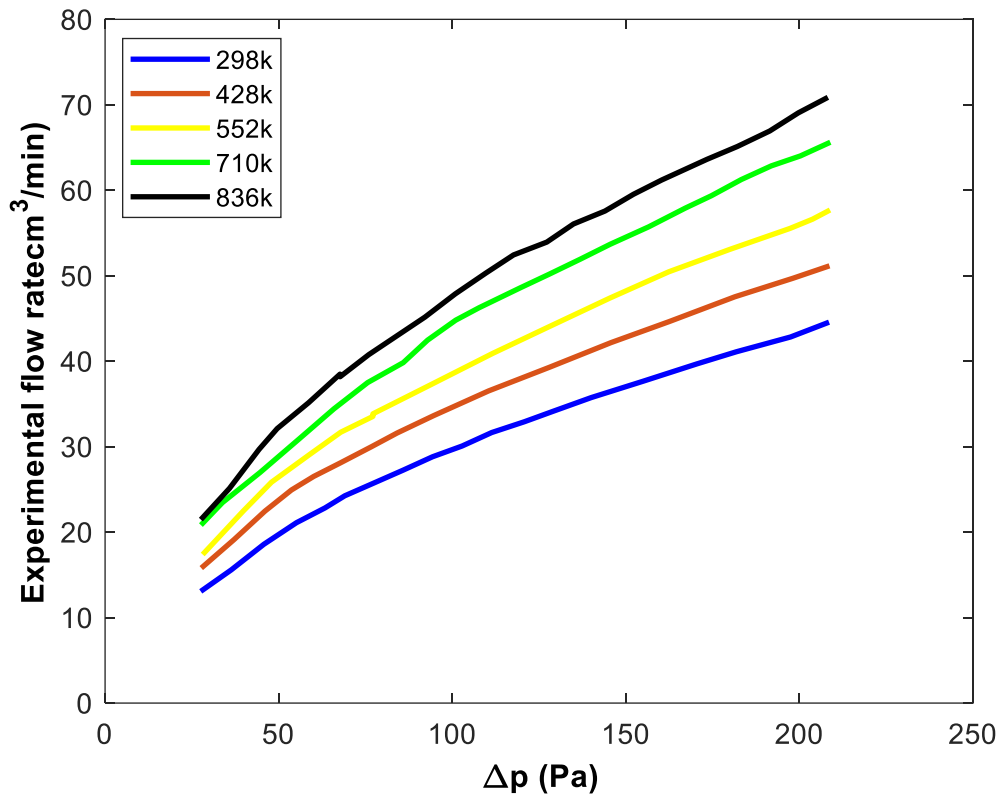


Figure 3.9: Experimental Flow rate through orifice versus differential pressure across orifice for 250 μ m

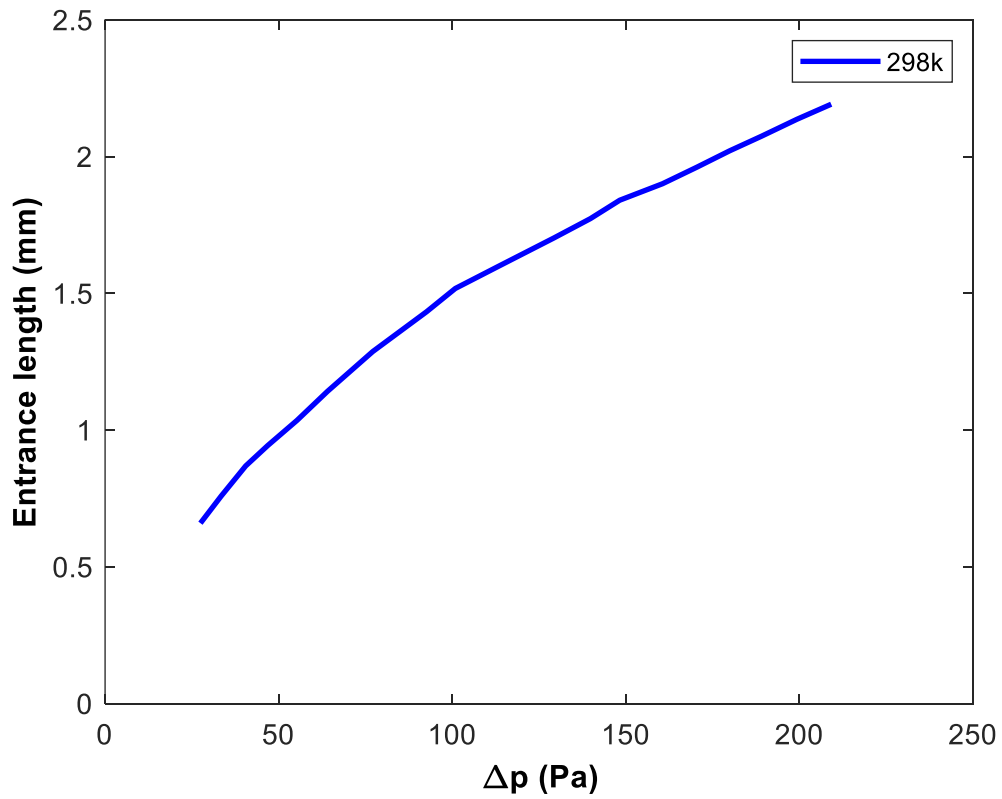


Figure 3.10: Variation of entrance length of ow through 250μm orifice with variation
in pressure across orifice

[113] did a study and considered the flow as fully developed but, in this case, it was discovered that the flow through the orifice is not fully developed as the orifice diameter (250μm) is comparable to the thickness of the wall surrounding the orifice (150μm). The entrance length of the flow with variation in suction pressure is calculated at temperature 298K and plotted in Fig. 3.10. This demonstrates that the entrance length is larger than the thickness of the wall and thus stating that the flow is still developing. The reason for this difference is likely due to the thickness of the wall surrounding the orifice which was reported by [113] was 0.7mm.

$$Q_o = A(c_1 \frac{\Delta P}{T^{0.8}} + c_2 T^{\frac{1}{2}} \Delta P^{\frac{1}{2}}) \quad (3.6)$$

where c_1 and c_2 are the calibration constant found to be 0.8 and 0.054 for the orifice diameter of 250μm and A is the cross-sectional area of orifice. Our calibration showed that flow velocity through orifice (and therefore, flow rate (Q_o)) is only the function of temperature and differential pressure across orifice as reported by Eq. 3.6. The equation consists of two terms, the first term is dependent on the velocity on gas viscosity and collision cross-section. While the second term is due to Bernoulli's equation for developing flow.

The experimental flow rate and the calibrated flow rate through the orifice for the case of 250μm is presented in Fig. 3.11. Both flow rates show agreement, as shown in fig 3.11.

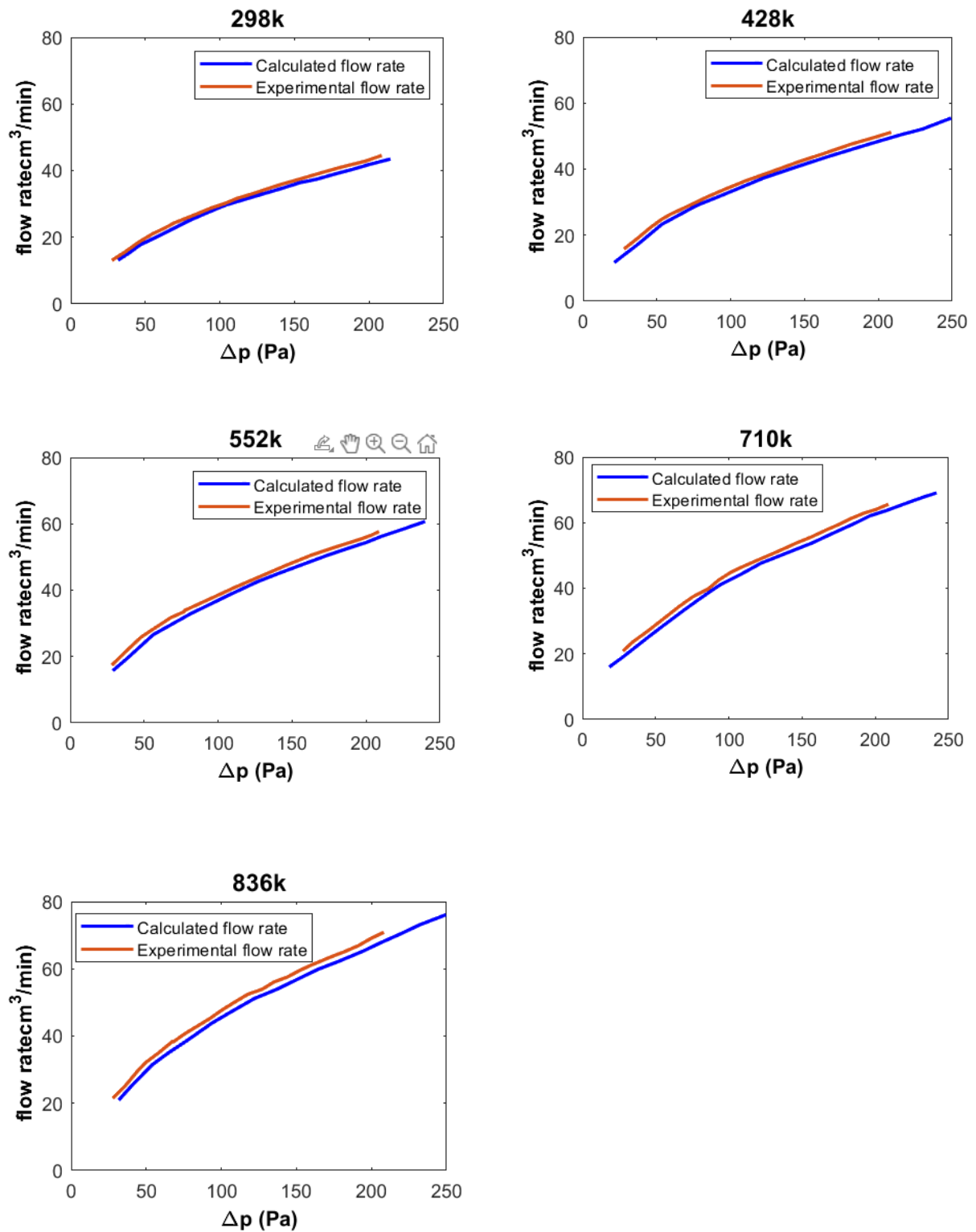


Figure 3.11: Comparison of experimental flow rate and calculated flow rate through orifice as a function of differential pressure across orifice for 250 μm diameter for different temperatures.

3.4 Summary

The detailed experimental set-up including the probe sampling and the atmospheric MFTR was described in this chapter. The theory of operation of particle sizer (SMPS) used in this study to measure soot particles was also described in this chapter. It was reported in earlier studies that mobility diameter measured by SMPS is limited in its accuracy for nano-sized particles and was, therefore, corrected to improve the accuracy. The flow rate through the sampling probe orifice was calibrated for 250 μ m orifice diameters. The orifice flow rate was used to calculate the dilution ratio between the carrier nitrogen gas and the incoming hot gases as reported later.

4. RESULTS AND DISCUSSIONS

In this section the experimental data obtained from the different conditions studied are carefully analyzed and then the appropriate plots are presented that help visualize the significance of the data.

4.1 Novel flow configuration for soot nucleation and oxidation investigations

The basic concept adapted here is to first mix fuel with thermal carrier bath (eg. N_2 with or without O_2) and preheat to a desired temperature to generate soot (see Fig. 4.1) in a laminar flow reactor. Once soot is formed in the first half of the reactor (depending on the target nominal residence time, temperature, fuel type, oxygen addition), controlled amounts of preheated secondary O_2 could be added via side tubes to start the soot oxidation process as shown in Fig. 4.1. The residence time in the second half of the reactor can be controlled to vary the soot particle size distribution emanating from the reactor and quantified via the SMPS placed at the exit of the reactor.

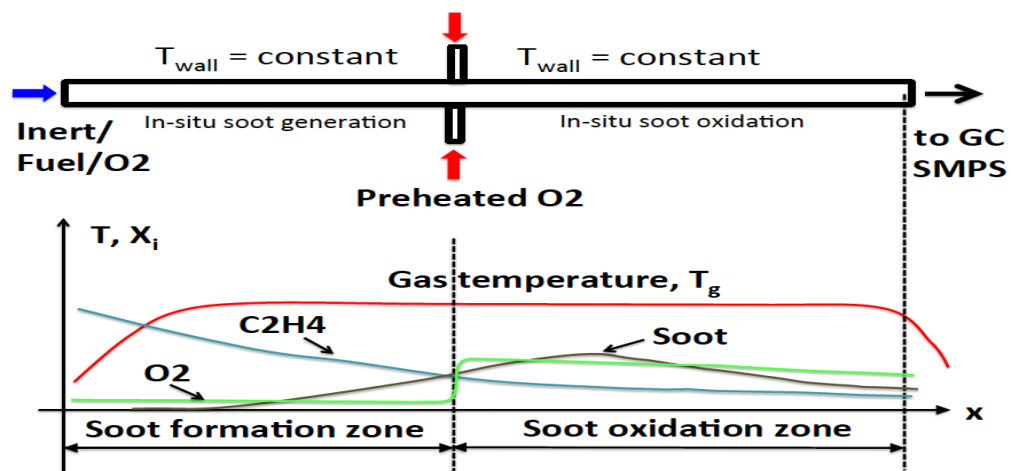


Figure 4.1: New reactor configuration adapted to study in-situ soot formation/oxidation at UVa.

While considerable sooting data exists in the literature with flow reactor experiments using ethylene as the fuel, such data is lacking for Jet fuels. After considerable exploration, the optimum rate controlling experimental conditions for Jet fuels at atmospheric pressure were

determined using the following conditions: Temperature: 900-1050 °C, Residence times: 80-160 ms, Main N₂ flow rate (for 160 ms):600 sccm, Jet fuel flow rate (for 80-160 ms):0.01 ml/min, Side-arm O₂ or N₂ flow rates:8 sccm .

The above listed conditions were found to be most sensitive for soot nucleation and oxidation with a range of jet fuels selected, namely “nominal” Jet A (A2 – POSF 10325, with Cetane # 48), Alternative Jet Fuel (AJF) C1 (POSF 11498 12368 with Cetane # 17.1) and C5 (POSF 12345, with Cetane # 39.6) [Colket et al., 2016]. AJF’s were considered by the National Jet Fuels Combustion program to understand the effects of bioderived SAF fuels on various combustion properties. (Note: at high pressures, the above flow reactor operating conditions may have to be tweaked to find optimum rate controlling conditions that are useful for model validation).

4.2 Soot Data with Jet A (POSF 10325) Pyrolysis and Oxidation

Petroleum derived “nominal” Jet A (POSF 10325) fuel consists of a broad range of molecules, from C7 to C18, with Fig. 4.2 showing the soot particle size distribution (PSD) obtained as a function of the overall reactor residence time (with N₂ addition from side-arm) and temperature. Results clearly show the sensitivity to temperature in conditions selected, with the highest soot production at 1050 °C (i.e., at the maximum temperature investigated here). The PSD’s also show that at these conditions mostly primary particles are formed with median size of about 20-25 microns, indicating low particle coagulation, especially at 1000 °C or below, for which was the desired goal.

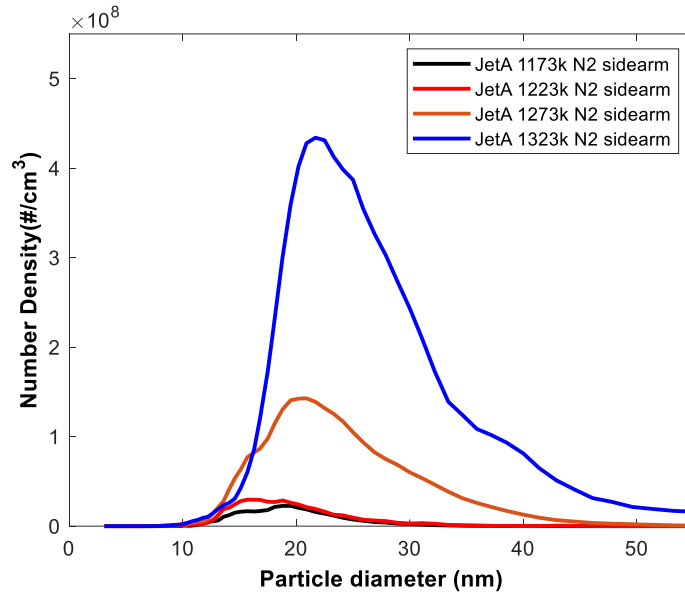


Figure 4.2: Soot PSD with Jet A (10325) as a function of the hot section temperature (900-1050 °C), for 160 ms, 1 atm, and 8 sccm of N₂ flow through sidearms.

Figure 4.3 shows the impact of replacing N₂ introduced through the side-arms with pure O₂ for a hot section temperature of 1050 °C, overall residence time of 160 ms, and 1 atm. The results show a profound effect on the soot PSD due to the presence of excess O₂ corresponding to lower equivalence ratio in the downstream section of the reactor (i.e., from equivalence ratio equal infinity (∞) at the inlet to equivalence ratio of 0.5). This change is due to two factors, rapid depletion of soot precursors and soot oxidation, which can be explored via a detailed kinetic model.

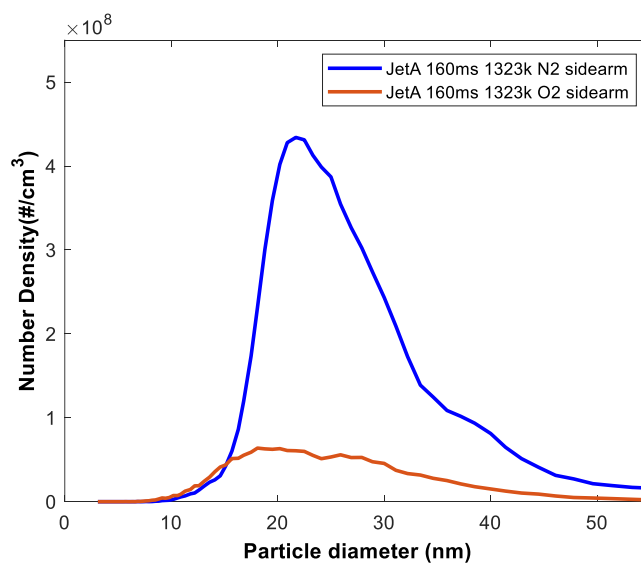


Figure 4.3: Soot PSD with Jet A (10325) with N₂ vs O₂ addition through the sidearms, for 160 ms, 1 atm, and 1050 °C.

Figure 4.4 shows the effect of residence time on soot PSD. The results clearly show that the residence time has a profound effect, indicating that the conditions selected are in rate controlling regime, i.e., the choice of chemical kinetic models will have a significant effect on model predictions. Furthermore, the soot PSD at 80 ms corresponds to case where soot production at the sidearm junction of 160 ms case. Thus, the differences seen between soot PSD at 160 ms with O₂ addition through sidearms (Fig. 4.3 red line) compared to the 80 ms case with N₂ addition (Fig. 4.4 black line) can be attributed to soot oxidation kinetics.

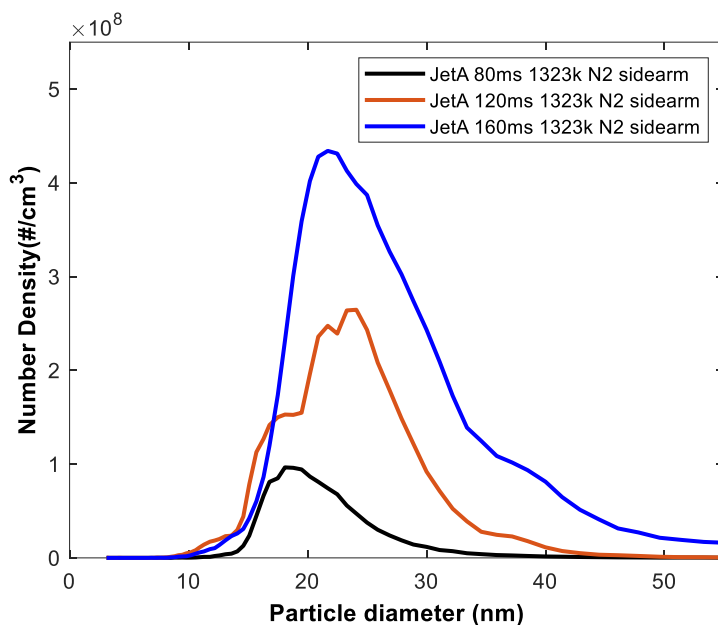


Figure 4.4: Effect of residence time on soot PSD at 1050 °C, 1 atm, and with 8 sccm N₂ addition through the sidearms.

The effect of O₂ addition with variation in reactor residence time can be seen in Figs. 4.3, 4.5 and 4.6. From these results, O₂ addition has the most impact on observed PSD at the highest residence time of 160 ms. Whether this effect is due to soot oxidation or depletion of soot precursors needs to be analyzed via chemical kinetic models. In short, with well-defined inflow conditions as presented here, numerical simulations can be performed to develop kinetic models of various level of complexity and address the applicability of current soot oxidation models, which is beyond the scope of the present work.

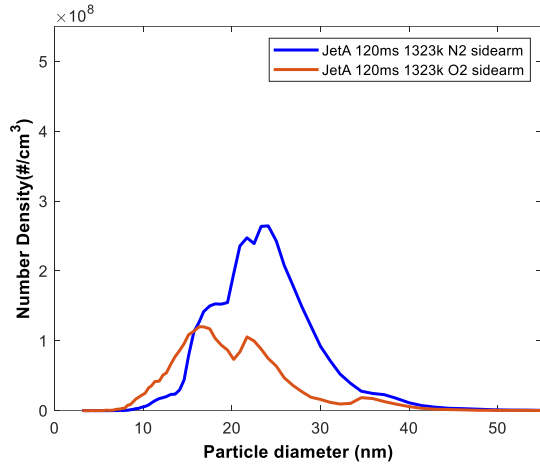


Figure 4.5: Effect of O₂ vs N₂ addition at 120 ms residence time with hot section at 1050 °C, 1 atm.

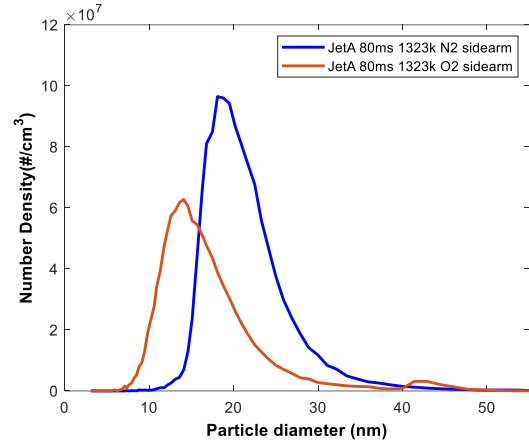


Figure 4.6: Effect of O₂ vs N₂ addition at 80 ms residence time with hot section at 1050 °C, 1 atm.

4.3 Soot Data with Alternate Jet Fuels C1 (POSF 11498) and C5 (PSOF 12345)

As mentioned above, in addition to “nominal” Jet A fuel, the soot PSD with several alternate jet fuels were also explored. These fuels are supposed to mimic new bio-derived sustainable aviation fuels being developed for civil aviation applications. Figures 4.7 and 4.8 show a comparison of soot PSD without and with O₂ addition for a reactor residence time of 160 ms, 1050 °C, and 1 atm. They clearly show a profound effect of sooting tendency with the selection fuel, including addition of secondary O₂ in the flow path.

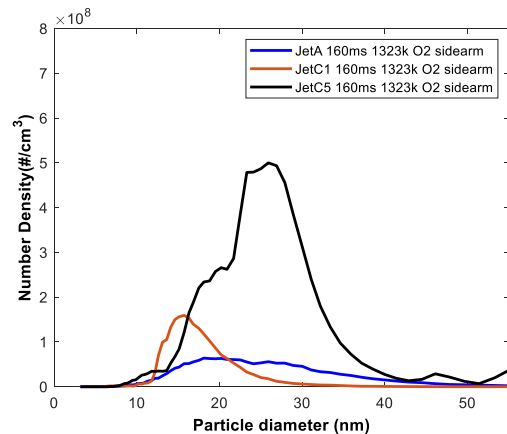
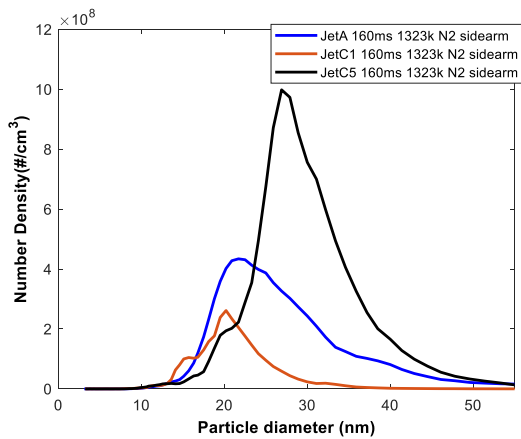


Figure 4.7: Comparison of soot PSD with different jet fuels N₂ addition from the sidearms, for 160 ms, 1050 °C, and 1 atm. Figure 4.8: Same as Fig. 4.6 but with O₂ addition from the sidearms.

4.4 Summary: Data based on the distinction between C1 and C5

Jet C1 (C₁₃H₂₈) and Jet C5 (C₁₀H₁₉) hydrocarbons are distinct from each other in terms of their molecular structures and properties. These distinctions have implications for oxidation and pyrolysis processes, as well as particle diameter.

Jet C1, with a molecular formula of C₁₃H₂₈, is a higher molecular weight hydrocarbon compared to Jet C5, which has a molecular formula of C₁₀H₁₉. This difference in molecular weight affects their physical and chemical characteristics.

In terms of oxidation, Jet C1 is more resistant to oxidation due to its larger molecular size. The additional carbon atoms and hydrogen atoms in its structure provide more stability and hinder the oxidation process. On the other hand, Jet C5 is more prone to oxidation due to its smaller molecular size, which allows for easier access of oxygen molecules to its carbon-carbon bonds. During pyrolysis, the process of thermal decomposition of hydrocarbons in the absence of oxygen, both Jet C1 and Jet C5 undergo cracking and produce soot. However, their molecular differences lead to variations in the composition and characteristics of the resulting soot. Jet C1 tends to produce larger and more complex soot particles compared to Jet C5. The higher molecular weight of Jet C1 leads to the formation of larger aromatic structures, resulting in larger particle diameters.

In contrast, Jet C5, being a smaller hydrocarbon, generates smaller and less complex soot particles during pyrolysis. The lower molecular weight of Jet C5 limits the size and complexity of the aromatic structures formed, leading to smaller particle diameters.

5. CONCLUSION

This study involves the experimental investigation of soot formation and oxidation in sustainable fuels. Several techniques have been employed in measuring particle size distribution functions in time past. But in this work, scanning mobility particle sizer was used. The particle size range for the SMPS used for this study measures particles of size 3nm to 105nm at standard operating conditions. The SMPS uses a sampling probe to draw particles into the flow region. Usually, the flow rate is dependent on the thickness of the probe tube wall and the diameter of the orifice. The thickness and orifice were selected based on literature and

was verified to be the optimum parameters for obtaining the reported particle size distribution data. In this study, a dilution ratio of about 2000 was used, which was necessary for preventing the agglomeration of soot particles in sampling line. The possible particle agglomeration can be neglected by the fact that the mean particle size range observed throughout the experiments ranged from 20 to 25 micron indicating only primary particles were formed.

An extensive set of experiments have been performed to provide soot oxidation rate in PSDF under conditions of oxidation and pyrolysis. A residence time of the range 80ms to 160ms over a temperature of 1173k to 1323k. The pressure for this experiment was kept at atmospheric pressure.

The results showed that the particle size distributions during the pyrolysis and oxidation of the alternate fuels were normally distributed. Additionally, the number density of soot particles increased with longer flow residence times at a constant temperature for the different temperature and residence time considered in this work. The result showed that there is profound effect of sooting tendency with the selection fuel (Jet A vs Alternate Jet Fuels C1, C5), including addition of secondary oxygen into the flow path. It was also seen in the work that 160ms seem to have the highest PSD, this is likely due to the longer allowed for proper mixing and combustion; thereby allowing for significant effect to take place. Similar results were seen across the selected fuels used in this work. It was observed that the experiment was very sensitive to temperature and as such the highest temperature (1050°C) showed the highest PSD in the work.

5.1 Future works

Although significant progress was made in trying to understand soot formation and the resulting size distribution function for the atmospheric pressure case, but the major aim of this

study was to see how these conditions used for the atmospheric pressure case affects the high-pressure case. So, we set out to build the high vessel. Due to the unavailability of some component parts, we were unable to run the high-pressure case. It is proposed that this high-pressure case is investigated with a view to seeing its effect on PSDF.

REFERENCES

1. Ali, S., Wu, X., Zuhra, Z., Ma, Y., Abbas, Y., Jin, B., Ran, R., & Weng, D. (2023). Cu-Mn-Ce mixed oxides catalysts for soot oxidation and their mechanistic chemistry. *Applied Surface Science*, 512, 145602. <https://doi.org/10.1016/j.apsusc.2020.145602>
2. Azam, N. A. M., Uemura, Y., Kusakabe, K., & Bustam, M. A. (2016). Biodiesel Production from Palm Oil Using Micro Tube Reactors: Effects of Catalyst Concentration and Residence Time. *Procedia Engineering*, 148, 354–360. <https://doi.org/10.1016/j.proeng.2016.06.462>
3. Baltzopoulou, P., Melas, A. D., Vlachos, N., Deloglou, D., Papaioannou, E., & Konstandopoulos, A. G. (2019). Solid Nucleation Mode Engine Exhaust Particles

- Detection at High Temperatures with an Advanced Half Mini DMA. *SAE Technical Paper Series*, 2(2). <https://doi.org/10.4271/2019-24-0052>
4. Banakar, V. V., Sabnis, S. S., Gogate, P. R., Raha, A., & Saurabh. (2022). Ultrasound assisted continuous processing in microreactors with focus on crystallization and chemical synthesis: A critical review. *Chemical Engineering Research and Design*, 182, 273–289. <https://doi.org/10.1016/j.cherd.2022.03.049>
 5. Bertolino, A., Stagni, A., Cuoci, A., Faravelli, T., Parente, A., & Frassoldati, A. (2019). Prediction of flammable range for pure fuels and mixtures using detailed kinetics. *Combustion and Flame*, 207, 120–133. <https://doi.org/10.1016/j.combustflame.2019.05.036>
 6. Betrancourt, C., Mercier, X., Liu, F., & Desgroux, P. (2019). Quantitative measurement of volume fraction profiles of soot of different maturities in premixed flames by extinction-calibrated laser-induced incandescence. *Applied Physics B*, 125(1). <https://doi.org/10.1007/s00340-018-7127-2>
 7. Bladh, H., Johnsson, J., & Bengtsson, P.-E. . (2009). Influence of spatial laser energy distribution on evaluated soot particle sizes using two-colour laser-induced incandescence in a flat premixed ethylene/air flame. *Applied Physics B*, 96(4), 645–656. <https://doi.org/10.1007/s00340-009-3523-y>
 8. Boyette, W., Chowdhury, S., & Roberts, W. (2017). Soot Particle Size Distribution Functions in a Turbulent Non-Premixed Ethylene-Nitrogen Flame. *Flow, Turbulence and Combustion*, 98(4), 1173–1186. <https://doi.org/10.1007/s10494-017-9802-5>
 9. Burandt, T., Xiong, B., Löffler, K., & Oei, P.-Y. (2019). Decarbonizing China’s energy system – Modeling the transformation of the electricity, transportation, heat, and industrial sectors. *Applied Energy*, 255, 113820. <https://doi.org/10.1016/j.apenergy.2019.113820>
 10. Carbone, F., Moslih, S., & Gomez, A. (2017). Probing gas-to-particle transition in a moderately sooting atmospheric pressure ethylene/air laminar premixed flame. Part II:

- Molecular clusters and nascent soot particle size distributions. *Combustion and Flame*, 181, 329–341. <https://doi.org/10.1016/j.combustflame.2017.02.021>
11. Cenker, E., Bruneaux, G., Dreier, T., & Schulz, C. (2014). Determination of small soot particles in the presence of large ones from time-resolved laser-induced incandescence. *Applied Physics B*, 118(2), 169–183. <https://doi.org/10.1007/s00340-014-5966-z>
 12. Chang, Y.-C., Lee, W.-J., Wu, T. S., Wu, C.-Y., & Chen, S.-J. (2014). Use of water containing acetone–butanol–ethanol for NO_x-PM (nitrogen oxide-particulate matter) trade-off in the diesel engine fueled with biodiesel. *Energy*, 64, 678–687. <https://doi.org/10.1016/j.energy.2013.10.077>
 13. Chen, J., & Pang, Z. (2021). Catalytically stabilized combustion characteristics of methane-air mixtures in micro-scale heat-recirculating systems. *Fuel*, 306, 121693. <https://doi.org/10.1016/j.fuel.2021.121693>
 14. Chen, Y., & Lin, B. (2021). Understanding the green total factor energy efficiency gap between regional manufacturing—insight from infrastructure development. *Energy*, 237, 121553. <https://doi.org/10.1016/j.energy.2021.121553>
 15. Choi, S., Myung, C. L., & Park, S. (2014). Review on characterization of nano-particle emissions and PM morphology from internal combustion engines: Part 2. *International Journal of Automotive Technology*, 15(2), 219–227. <https://doi.org/10.1007/s12239-014-0023-9>
 16. Chu, H., Han, W., Cao, W., Gu, M., & Xu, G. (2019). Effect of methane addition to ethylene on the morphology and size distribution of soot in a laminar co-flow diffusion flame. *Energy*, 166, 392–400. <https://doi.org/10.1016/j.energy.2018.10.093>
 17. Chu, H., Ya, Y., Nie, X., Qiao, F., & E, J. (2021). Effects of adding cyclohexane, n-hexane, ethanol, and 2,5-dimethylfuran to fuel on soot formation in laminar coflow n-heptane/iso-octane diffusion flame. *Combustion and Flame*, 225, 120–135. <https://doi.org/10.1016/j.combustflame.2020.10.030>

18. Commodo, M., Karataş, A. E., De Falco, G., Minutolo, P., D'Anna, A., & Gülder, Ö. L. (2020). On the effect of pressure on soot nanostructure: A Raman spectroscopy investigation. *Combustion and Flame*, *219*, 13–19. <https://doi.org/10.1016/j.combustflame.2020.04.008>
19. Cornette, J. F. P., Blondeau, J., & Bram, S. (2023). Influence of the dynamic behaviour of impactor surfaces on particulate matter emission measurements with electrical low pressure impactors. *Powder Technology*, *419*, 118333. <https://doi.org/10.1016/j.powtec.2023.118333>
20. Dandajeh, H. A., Ladommatos, N., & Hellier, P. (2020). Influence of unsaturation of hydrocarbons on the characteristics and carcinogenicity of soot particles. *Journal of Analytical and Applied Pyrolysis*, *151*, 104900. <https://doi.org/10.1016/j.jaap.2020.104900>
21. Dong, Z., Wen, Z., Zhao, F., Kuhn, S., & Noël, T. (2021). Scale-up of micro- and milli-reactors: An overview of strategies, design principles and applications. *Chemical Engineering Science: X*, *10*, 100097. <https://doi.org/10.1016/j.cesx.2021.100097>
22. Dziubak, T., & Dziubak, S. D. (2022). A Study on the Effect of Inlet Air Pollution on the Engine Component Wear and Operation. *Energies*, *15*(3), 1182. <https://doi.org/10.3390/en15031182>
23. Farhan, S. M., & Wang, P. (2022). Post-injection strategies for performance improvement and emissions reduction in DI diesel engines—A review. *Fuel Processing Technology*, *228*, 107145. <https://doi.org/10.1016/j.fuproc.2021.107145>
24. Ferraro, F., Gierth, S., Salenbauch, S., Han, W., & Hasse, C. (2022). Soot particle size distribution reconstruction in a turbulent sooting flame with the split-based extended quadrature method of moments. *Physics of Fluids*, *34*(7), 075121. <https://doi.org/10.1063/5.0098382>
25. Gaetano Esposito. private communication, 2014.
26. Hagen, F., Hardock, F., Koch, S., Sebbar, N., Bockhorn, H., Loukou, A., Kubach, H., Suntz, R., Trimis, D., & Koch, T. (2020). Why Soot is not Alike Soot: A

Molecular/Nanostructural Approach to Low Temperature Soot Oxidation. *Flow, Turbulence and Combustion*, 106(2), 295–329. <https://doi.org/10.1007/s10494-020-00205-2>

27. Henderson, L., Shukla, P., Rudolph, V., & Bhatia, S. K. (2022). Modelling the formation, growth and coagulation of soot in a combustion system using a 2-D population balance model. *Combustion and Flame*, 245, 112303. <https://doi.org/10.1016/j.combustflame.2022.112303>
28. Hu, X., Yu, Z., Chen, L., Huang, Y., Zhang, C., Salehi, F., Chen, R., Harrison, R. M., & Xu, J. (2022). Morphological and nanostructure characteristics of soot particles emitted from a jet-stirred reactor burning aviation fuel. *Combustion and Flame*, 236, 111760. <https://doi.org/10.1016/j.combustflame.2021.111760>
29. Huo, Z., Cleary, M. J., Masri, A. R., & Mueller, M. E. (2022). A coupled MMC-LES and sectional kinetic scheme for soot formation in a turbulent flame. *Combustion and Flame*, 241, 112089. <https://doi.org/10.1016/j.combustflame.2022.112089>
30. Jeyaseelan, T., Ekambaram, P., Subramanian, J., & Shamim, T. (2022). A comprehensive review on the current trends, challenges and future prospects for sustainable mobility. *Renewable and Sustainable Energy Reviews*, 157, 112073. <https://doi.org/10.1016/j.rser.2022.112073>
31. Jiaqiang, E., Pham, M., Zhao, D., Deng, Y., Le, D., Zuo, W., Zhu, H., Liu, T., Peng, Q., & Zhang, Z. (2017). Effect of different technologies on combustion and emissions of the diesel engine fueled with biodiesel: A review. *Renewable and Sustainable Energy Reviews*, 80, 620–647. <https://doi.org/10.1016/j.rser.2017.05.250>
32. Jiaqiang, E., Xu, W., Ma, Y., Tan, D., Peng, Q., Tan, Y., & Chen, L. (2022). Soot formation mechanism of modern automobile engines and methods of reducing soot emissions: A review. *Fuel Processing Technology*, 235, 107373. <https://doi.org/10.1016/j.fuproc.2022.107373>

33. K Erickson, M Singh, and B Osmondson. Measuring nanoparticle size distributions in real-time: Key factors for accuracy.
34. Kalvakala, K. C., Katta, V. R., & Aggarwal, S. K. (2018). Effects of oxygen-enrichment and fuel unsaturation on soot and NO_x emissions in ethylene, propane, and propene flames. *Combustion and Flame*, 187, 217–229. <https://doi.org/10.1016/j.combustflame.2017.09.015>
35. Kamada, T., Nakamura, H., Tezuka, T., Hasegawa, S., & Maruta, K. (2014). Study on combustion and ignition characteristics of natural gas components in a micro flow reactor with a controlled temperature profile. *Combustion and Flame*, 161(1), 37–48. <https://doi.org/10.1016/j.combustflame.2013.08.013>
36. Kempema, N. J., & Long, M. B. (2016). Combined optical and TEM investigations for a detailed characterization of soot aggregate properties in a laminar coflow diffusion flame. *Combustion and Flame*, 164, 373–385. <https://doi.org/10.1016/j.combustflame.2015.12.001>
37. Kholghy, M. R., Afarin, Y., Sediako, A. D., Barba, J., Lapuerta, M., Chu, C., Weingarten, J., Borshanjpour, B., Chernov, V., & Thomson, M. J. (2017). Comparison of multiple diagnostic techniques to study soot formation and morphology in a diffusion flame. *Combustion and Flame*, 176, 567–583. <https://doi.org/10.1016/j.combustflame.2016.11.012>
38. Kohse-Höinghaus, K. (2020). Combustion in the future: The importance of chemistry. *Proceedings of the Combustion Institute. International Symposium on Combustion*, 38(1). <https://doi.org/10.1016/j.proci.2020.06.375>
39. Krishnamoorthi, M., Sreedhara, S., & Duvvuri, P. P. (2021). The effect of low reactivity fuels on the dual fuel mode compression ignition engine with exergy and soot analyses. *Fuel*, 290, 120031. <https://doi.org/10.1016/j.fuel.2020.120031>

40. La Rocca, A., Di Liberto, G., Shayler, P. J., Parmenter, C. D. J., & Fay, M. W. (2014). Application of nanoparticle tracking analysis platform for the measurement of soot-in-oil agglomerates from automotive engines. *Tribology International*, *70*, 142–147. <https://doi.org/10.1016/j.triboint.2013.09.018>
41. Lee, H., Yook, S.-J., & Ahn, K.-H. (2020). Effects of exponentially decaying and growing concentrations on particle size distribution from a scanning mobility particle sizer. *Aerosol Science and Technology*, *54*(10), 1135–1143. <https://doi.org/10.1080/02786826.2020.1761538>
42. Lei, X., Wang, Y., & Liu, D. (2021). Effects of oxygenated biofuel additives on soot formation: A comprehensive review of laboratory-scale studies. *Fuel*, *313*. <https://doi.org/10.1016/j.fuel.2021.122635>
43. Lemmens, A. K., Rap, D. B., Thunnissen, J. M. M., Willemsen, B., & Rijs, A. M. (2020). Polycyclic aromatic hydrocarbon formation chemistry in a plasma jet revealed by IR-UV action spectroscopy. *Nature Communications*, *11*(1), 269. <https://doi.org/10.1038/s41467-019-14092-3>
44. Liu, J., Wu, P., Sun, P., Ji, Q., Zhang, Q., & Wang, P. (2021). Effects of iron-based fuel borne catalyst addition on combustion, in-cylinder soot distribution and exhaust emission characteristics in a common-rail diesel engine. *Fuel*, *290*, 120096. <https://doi.org/10.1016/j.fuel.2020.120096>
45. Liu, L., Xu, H., Zhu, Q., Ren, H., & Li, X. (2020). Soot formation of n-decane pyrolysis: A mechanistic view from ReaxFF molecular dynamics simulation. *Chemical Physics Letters*, *760*, 137983. <https://doi.org/10.1016/j.cplett.2020.137983>
46. Lou, C., Li, Z., Zhang, Y., & Kumfer, B. M. (2021). Soot formation characteristics in laminar coflow flames with application to oxy-combustion. *Combustion and Flame*, *227*, 371–383. <https://doi.org/10.1016/j.combustflame.2021.01.018>
47. M Knudsen and S Weber. Resistance to motion of small spheres. *Ann. Phys*, *36* (5):981{994, 1911.

48. Malmborg, V. B., Eriksson, A. C., Shen, M., Nilsson, P., Gallo, Y., Waldheim, B., Martinsson, J., Andersson, Ö., & Pagels, J. (2017). Evolution of In-Cylinder Diesel Engine Soot and Emission Characteristics Investigated with Online Aerosol Mass Spectrometry. *Environmental Science & Technology*, 51(3), 1876–1885. <https://doi.org/10.1021/acs.est.6b03391>
49. Mao, Q., & Luo, K. H. (2019). Trace metal assisted polycyclic aromatic hydrocarbons fragmentation, growth and soot nucleation. *Proceedings of the Combustion Institute*, 37(1), 1023–1030. <https://doi.org/10.1016/j.proci.2018.06.106>
50. Mao, Q., van Duin, A. C. T., & Luo, K. H. (2017). Formation of incipient soot particles from polycyclic aromatic hydrocarbons: A ReaxFF molecular dynamics study. *Carbon*, 121, 380–388. <https://doi.org/10.1016/j.carbon.2017.06.009>
51. Martin, J. W., Salamanca, M., & Kraft, M. (2022). Soot inception: Carbonaceous nanoparticle formation in flames. *Progress in Energy and Combustion Science*, 88, 100956. <https://doi.org/10.1016/j.pecs.2021.100956>
52. Mei, J., Zhou, Y., You, X., & Law, C. K. (2021). Formation of nascent soot during very fuel-rich oxidation of ethylene at low temperatures. *Combustion and Flame*, 226, 31–41. <https://doi.org/10.1016/j.combustflame.2020.11.031>
53. Meng, Y., Zhang, Z., Yin, H., & Ma, T. (2018). Automatic detection of particle size distribution by image analysis based on local adaptive canny edge detection and modified circular Hough transform. *Micron*, 106, 34–41. <https://doi.org/10.1016/j.micron.2017.12.002>
54. Michael D Allen and Otto G Raabe. Slip correction measurements of spherical solid aerosol particles in an improved millikan apparatus. *Aerosol Science and Technology*, 4(3):269{286, 1985.
55. Morajkar, P. P., Abdrabou, M. K., Raj, A., Elkadi, M., Stephen, S., & Ibrahim Ali, M. (2020). Transmission of trace metals from fuels to soot particles: An ICP-MS and soot

- nanostructural disorder study using diesel and diesel/Karanja biodiesel blend. *Fuel*, 280, 118631. <https://doi.org/10.1016/j.fuel.2020.118631>
56. Morán, J., Poux, A., & Yon, J. (2021). Impact of the competition between aggregation and surface growth on the morphology of soot particles formed in an ethylene laminar premixed flame. *Journal of Aerosol Science*, 152, 105690. <https://doi.org/10.1016/j.jaerosci.2020.105690>
57. Nadezhda A Slavinskaya, Uwe Riedel, Seth B Dworkin, and Murray J Thomson. Detailed numerical modeling of pah formation and growth in non-premixed ethylene and ethane flames. *Combustion and Flame*, 159(3):979{995, 2012.
58. Naseri, A., Veshkini, A., & Thomson, M. J. (2017). Detailed modeling of CO₂ addition effects on the evolution of soot particle size distribution functions in premixed laminar ethylene flames. *Combustion and Flame*, 183, 75–87. <https://doi.org/10.1016/j.combustflame.2017.04.028>
59. Niemelä, N. P., Mylläri, F., Kuittinen, N., Aurela, M., Helin, A., Kuula, J., Teinilä, K., Nikka, M., Vainio, O., Arffman, A., Lintusaari, H., Timonen, H., Rönkkö, T., & Joronen, T. (2022). Experimental and numerical analysis of fine particle and soot formation in a modern 100 MW pulverized biomass heating plant. *Combustion and Flame*, 240, 111960. <https://doi.org/10.1016/j.combustflame.2021.111960>
60. Nobili, A., Cuoci, A., Pejpichestakul, W., Pelucchi, M., Cavallotti, C., & Faravelli, T. (2022). Modeling soot particles as stable radicals: a chemical kinetic study on formation and oxidation. Part I. Soot formation in ethylene laminar premixed and counterflow diffusion flames. *Combustion and Flame*, 243, 112073. <https://doi.org/10.1016/j.combustflame.2022.112073>
61. Oh, K. C., Lee, C. B., & Lee, E. J. (2011). Characteristics of soot particles formed by diesel pyrolysis. *Journal of Analytical and Applied Pyrolysis*, 92(2), 456–462. <https://doi.org/10.1016/j.jaap.2011.08.009>
62. Operation and service manual for Nano water-based condensation particle counter

63. Ouf, F. X., Yon, J., Ausset, P., Coppalle, A., & Maillé, M. (2010). Influence of Sampling and Storage Protocol on Fractal Morphology of Soot Studied by Transmission Electron Microscopy. *Aerosol Science and Technology*, *44*(11), 1005–1017. <https://doi.org/10.1080/02786826.2010.507228>
64. Pacino, A., La Porta, C., La Rocca, A., & Cairns, A. (2023). Copper leaching effects on combustion characteristics and particulate emissions of a direct injection high pressure common rail diesel engine. *Fuel*, *340*, 127536. <https://doi.org/10.1016/j.fuel.2023.127536>
65. Park, S. H. (2022). Bi-modal moment model for predicting the formation and growth of soot aggregate particles. *Particulate Science and Technology*, *41*(1), 22–31. <https://doi.org/10.1080/02726351.2022.2029990>
66. Park, S., Wang, Y., Chung, S. H., & Sarathy, S. M. (2017). Compositional effects on PAH and soot formation in counterflow diffusion flames of gasoline surrogate fuels. *Combustion and Flame*, *178*, 46–60. <https://doi.org/10.1016/j.combustflame.2017.01.001>
67. PB Keady, FR Quant, and GJ Sem. A condensation nucleus counter for clean rooms. *Proc. Institute of Environmental Sci., Annual Technical Mtg*, pages 445{451, 1986.
68. Reizer, E., Viskolcz, B., & Fiser, B. (2022). Formation and growth mechanisms of polycyclic aromatic hydrocarbons: A mini-review. *Chemosphere*, *291*, 132793. <https://doi.org/10.1016/j.chemosphere.2021.132793>
69. Ren, F., Cheng, X., Gao, Z., Huang, Z., & Zhu, L. (2023). Effects of NH₃ addition on polycyclic aromatic hydrocarbon and soot formation in C₂H₄ co-flow diffusion flames. *Combustion and Flame*, *241*, 111958. <https://doi.org/10.1016/j.combustflame.2021.111958>
70. Rigopoulos, S. (2019). Modelling of Soot Aerosol Dynamics in Turbulent Flow. *Flow, Turbulence and Combustion*, *103*(3), 565–604. <https://doi.org/10.1007/s10494-019-00054-8>

71. Ruiz, M. P., de Villoria, R. G., Millera, A., Alzueta, M. U., & Bilbao, R. (2007). Influence of the temperature on the properties of the soot formed from C₂H₂ pyrolysis. *Chemical Engineering Journal*, 127(1-3), 1-9.
72. Saggese, C., Ferrario, S., Camacho, J., Cuoci, A., Frassoldati, A., Ranzi, E., Wang, H., & Faravelli, T. (2015). Kinetic modeling of particle size distribution of soot in a premixed burner-stabilized stagnation ethylene flame. *Combustion and Flame*, 162(9), 3356–3369. <https://doi.org/10.1016/j.combustflame.2015.06.002>
73. Samuel L Manzello, David B Lenhert, Ahmet Yozgatligil, Michael T Donovan, George W Mulholland, Michael R Zachariah, and Wing Tsang. Soot particle size distributions in a well-stirred reactor/plug flow reactor. *Proceedings of the Combustion Institute*, 31(1):675{683, 2007.
74. Shariatmadar, H., Aleiferis, P. G., & Lindstedt, R. P. (2022). Particle size distributions in turbulent premixed ethylene flames crossing the soot inception limit. *Combustion and Flame*, 243, 111978. <https://doi.org/10.1016/j.combustflame.2021.111978>
75. Sheng, H., Huang, X., Ji, Y., Zhao, Z., Hu, W., Chen, J., Ji, Z., Wang, X., & Liu, H. (2023). Soot emission reduction in n-hexadecane/cycloalkane mixtures combustion with the addition of Borane-dimethyl sulfide. *Fuel*, 321, 124098. <https://doi.org/10.1016/j.fuel.2022.124098>
76. Singh, P., Sharma, S., Almohammadi, B. A., Khandelwal, B., & Kumar, S. (2020). Applicability of aromatic selection towards newer formulated fuels for regulated and unregulated emissions reduction in CI engine. *Fuel Processing Technology*, 209, 106548. <https://doi.org/10.1016/j.fuproc.2020.106548>
77. Sirignano, M., Ghiassi, H., D'Anna, A., & Lighty, J. S. (2016). Temperature and oxygen effects on oxidation-induced fragmentation of soot particles. *Combustion and Flame*, 171, 15–26. <https://doi.org/10.1016/j.combustflame.2016.05.011>
78. Stefanidis, E. K., Ebaugh, T. A., Bliznakov, S., Bonville, L. J., Maric, R., & Carbone, F. (2022). Laser diagnostics to characterize the in-flame growth of platinum

- nanoparticles manufactured by the reactive spray deposition technology. *Combustion and Flame*, 246, 112412. <https://doi.org/10.1016/j.combustflame.2022.112412>
79. Stephen William Lasher. Ultra-fine soot investigation in flames. PhD thesis, Massachusetts Institute of Technology, 1999.
80. Sun, B., & Rigopoulos, S. (2022). Modelling of soot formation and aggregation in turbulent flows with the LES-PBE-PDF approach and a conservative sectional method. *Combustion and Flame*, 242, 112152. <https://doi.org/10.1016/j.combustflame.2022.112152>
81. Susanne V Hering, Mark R Stolzenburg, Frederick R Quant, Derek R Oberreit, and Patricia B Keady. A laminar flow, water-based condensation particle counter(wcpc). *Aerosol Science and Technology*, 39(7):659-672, 2005.
82. Tang, A., Xu, Y., Shan, C., Pan, J., & Liu, Y. (2015). A comparative study on combustion characteristics of methane, propane and hydrogen fuels in a micro-combustor. *International Journal of Hydrogen Energy*, 40(46), 16587–16596. <https://doi.org/10.1016/j.ijhydene.2015.09.101>
83. Trivanovic, U., Sipkens, T. A., Kazemimanesh, M., Baldelli, A., Jefferson, A. M., Conrad, B. M., Johnson, M. R., Corbin, J. C., Olfert, J. S., & Rogak, S. N. (2023). Morphology and size of soot from gas flares as a function of fuel and water addition. *Fuel*, 279, 118478. <https://doi.org/10.1016/j.fuel.2020.118478>
84. Vargas, A. M., & Gülder, Ö. L. (2016). A multi-probe thermophoretic soot sampling system for high-pressure diffusion flames. *Review of Scientific Instruments*, 87(5), 055101. <https://doi.org/10.1063/1.4947509>
85. Venvik, H. J., & Yang, J. (2017). Catalysis in microstructured reactors: Short review on small-scale syngas production and further conversion into methanol, DME and Fischer-Tropsch products. *Catalysis Today*, 285, 135–146. <https://doi.org/10.1016/j.cattod.2017.02.014>

86. Verma, P., Pickering, E., Jafari, M., Guo, Y., Stevanovic, S., Fernando, J. F. S., Golberg, D., Brooks, P., Brflown, R., & Ristovski, Z. (2019). Influence of fuel-oxygen content on morphology and nanostructure of soot particles. *Combustion and Flame*, 205, 206–219. <https://doi.org/10.1016/j.combustflame.2019.04.009>
87. Wang, C., Yuen, A. C. Y., Chan, Q. N., Chen, T. B. Y., Yang, W., Cheung, S. C. P., & Yeoh, G. H. (2020). Characterisation of soot particle size distribution through population balance approach and soot diagnostic techniques for a buoyant non-premixed flame. *Journal of the Energy Institute*, 93(1), 112–128. <https://doi.org/10.1016/j.joei.2019.04.004>
88. Wang, X., Gao, J., Chen, H., Chen, Z., Zhang, P., & Chen, Z. (2022). Diesel/methanol dual-fuel combustion: An assessment of soot nanostructure and oxidation reactivity. *Fuel Processing Technology*, 237, 107464. <https://doi.org/10.1016/j.fuproc.2022.107464>
89. Wang, Y., & Chung, S. H. (2019). Soot formation in laminar counterflow flames. *Progress in Energy and Combustion Science*, 74, 152–238. <https://doi.org/10.1016/j.pecs.2019.05.003>
90. Wang, Y., Gu, M., Zhu, Y., Cao, L., Zhu, B., Wu, J., Lin, Y., & Huang, X. (2021). A review of the effects of hydrogen, carbon dioxide, and water vapor addition on soot formation in hydrocarbon flames. *International Journal of Hydrogen Energy*, 46(61), 31400–31427. <https://doi.org/10.1016/j.ijhydene.2021.07.011>
91. Wang, Y., Liu, H., Mei, D., Wu, Q., & Zhou, H. (2021). A novel thermally autonomous methanol steam reforming microreactor using SiC honeycomb ceramic as catalyst support for hydrogen production. *International Journal of Hydrogen Energy*, 46(51), 25878–25892. <https://doi.org/10.1016/j.ijhydene.2021.05.103>

92. Wei, X., Gui, H., Liu, J., & Cheng, Y. (2022). Characterization of submicron aerosol particles in winter at Albany, New York. *Journal of Environmental Sciences*, *111*, 118–129. <https://doi.org/10.1016/j.jes.2021.03.004>
93. Williams C Hinds. *Aerosol technology: properties, behavior, and measurement of airborne particles*. New York, Wiley-Interscience, 1982. 442 p., 1, 1982.
94. Wong, P. K., Ghadikolaei, M. A., Chen, S. H., Fadairo, A. A., Ng, K. W., Lee, S. M. Y., Xu, J. C., Lian, Z. D., Li, L., Wong, H. C., Ning, Z., Gali, N. K., & Zhao, J. (2022). Physical, chemical, and cell toxicity properties of mature/aged particulate matter (PM) trapped in a diesel particulate filter (DPF) along with the results from freshly produced PM of a diesel engine. *Journal of Hazardous Materials*, *434*, 128855. <https://doi.org/10.1016/j.jhazmat.2022.128855>
95. . Wu, S., Yang, S., Tay, K. L., Yang, W., & Jia, M. (2022). A hybrid sectional moment projection method for discrete population balance dynamics involving inception, growth, coagulation and fragmentation. *Chemical Engineering Science*, *249*, 117333. <https://doi.org/10.1016/j.ces.2021.117333>
96. . Xu, L., Yan, F., Zhou, M., & Wang, Y. (2021). An experimental and modeling study on sooting characteristics of laminar counterflow diffusion flames with partial premixing. *Energy*, *218*, 119479. <https://doi.org/10.1016/j.energy.2020.119479>
97. . Yang, P.-M., Wang, C.-C., Lin, Y.-C., Jhang, S.-R., Lin, L.-J., & Lin, Y.-C. (2017). Development of novel alternative biodiesel fuels for reducing PM emissions and PM-related genotoxicity. *Environmental Research*, *156*, 512–518. <https://doi.org/10.1016/j.envres.2017.03.045>
98. .Yang, W., Pudasainee, D., Gupta, R., Li, W., Wang, B., & Sun, L. (2021). An overview of inorganic particulate matter emission from coal/biomass/MSW combustion: Sampling and measurement, formation, distribution, inorganic composition and influencing factors. *Fuel Processing Technology*, *213*, 106657. <https://doi.org/10.1016/j.fuproc.2020.106657>

99. Yao, X., Zhang, Y., Du, L., Liu, J., & Yao, J. (2015). Review of the applications of microreactors. *Renewable and Sustainable Energy Reviews*, *47*, 519–539. <https://doi.org/10.1016/j.rser.2015.03.078>
100. Zhang, C., Chen, L., Ding, S., Xu, H., Li, G., Consalvi, J.-L., & Liu, F. (2019). Effects of soot inception and condensation PAH species and fuel preheating on soot formation modeling in laminar coflow CH₄/air diffusion flames doped with n-heptane/toluene mixtures. *Fuel*, *253*, 1371–1377. <https://doi.org/10.1016/j.fuel.2019.05.100>
101. Zhang, C., Wu, Y., Liu, B., Wang, Z., & Zhou, L. (2022). Investigation of soot particles morphology and size distribution produced in a n-heptane/anisole laminar diffusion flame based on TEM images. *Combustion and Flame*, *244*, 112234. <https://doi.org/10.1016/j.combustflame.2022.112234>
102. Zhang, K., Xu, Y., Qin, L., Liu, Y., Wang, H., Liu, Y., & Cheng, X. (2022). Experimental and numerical study of soot volume fraction and number density in laminar co-flow diffusion flames of n-decane/n-butanol blends. *Fuel*, *330*, 125620. <https://doi.org/10.1016/j.fuel.2022.125620>
103. Zhang, P., Wu, H., Song, X., Liu, Y., & Cheng, X. (2022). Fuel molecular structure influences the polycyclic aromatic hydrocarbons formation of butanol/butane isomers: A ReaxFF molecular dynamics study. *Fuel*, *310*, 122460. <https://doi.org/10.1016/j.fuel.2021.122460>
104. Zhang, Z., Tian, J., Li, J., Cao, C., Wang, S., Lv, J., Zheng, W., & Tan, D. (2022). The development of diesel oxidation catalysts and the effect of sulfur dioxide on catalysts of metal-based diesel oxidation catalysts: A review. *Fuel Processing Technology*, *233*, 107317. <https://doi.org/10.1016/j.fuproc.2022.107317>
105. Zhao, B., Liang, X., Wang, K., Li, T., Lv, X., & Zhang, S. (2022). Impact of sulfur functional groups on physicochemical properties and oxidation reactivity of diesel soot particles. *Fuel*, *327*, 125041. <https://doi.org/10.1016/j.fuel.2022.125041>

106. Zhao, X., E, J., Liao, G., Zhang, F., Chen, J., & Deng, Y. (2021). Numerical simulation study on soot continuous regeneration combustion model of diesel particulate filter under exhaust gas heavy load. *Fuel*, 290, 119795. <https://doi.org/10.1016/j.fuel.2020.119795>
107. Zhigang Li and Hai Wang. Drag force, diffusion coefficient, and electric mobility of small particles. ii. application. *Physical Review E*, 68(6):061207, 2003.
108. EO Knutson and KT Whitby. Aerosol classification by electric mobility: apparatus, theory, and applications. *Journal of Aerosol Science*, 6(6):443{451, 1975.
109. Michael D Allen and Otto G Raabe. Slip correction measurements of spherical solid aerosol particles in an improved millikan apparatus. *Aerosol Science and Technology*, 4(3):269{286, 1985.
110. U Shrestha, GP Simms, CG Moniruzzaman, and HK Chelliah. High-pressure fuel pyrolysis investigation using a micro flow tube reactor. In 53rd AIAA Aerospace Sciences Meeting, Orlando, FL, 2015.
111. Bin Zhao, Kei Uchikawa, and Hai Wang. A comparative study of nanoparticles in premixed flames by scanning mobility particle sizer, small angle neutron scattering, and transmission electron microscopy. *Proceedings of the Combustion Institute*, 31(1):851(860, 2007).
112. Zhigang Li and Hai Wang. Drag force, diffusion coefficient, and electric mobility of 1. small particles. ii. application. *Physical Review E*, 68(6):061207, 2003.
113. Bin Zhao, Zhiwei Yang, Jinjin Wang, Murray V Johnston, and Hai Wang. Analysis of soot nanoparticles in a laminar premixed ethylene flame by scanning mobility particle sizer. *Aerosol Science & Technology*, 37(8):611{620, 2003}.
114. J. Guo, Y. Tang, V. Raman, and H. G. Im, "Numerical investigation of pressure effects on soot formation in laminar coflow ethylene/air diffusion flames," *Fuel*, vol. 292, p. 120176, May 2021, doi: <https://doi.org/10.1016/j.fuel.2021.120176>.
115. T. Agarwal, B. K. Sahoo, M. Kumar, and B. K. Sapra, "A Computational Fluid Dynamics code for aerosol and decay-product studies in indoor environments," *Journal of*

- Radioanalytical and Nuclear Chemistry*, vol. 330, no. 3, pp. 1347–1355, Jul. 2021, doi: <https://doi.org/10.1007/s10967-021-07877-8>.
116. A. X. Zheng, Sundar Manikandan, S. E. Wonfor, A. M. Steinberg, and Y. C. Mazumdar, “Planar time-resolved laser-induced incandescence for pressurized premixed Jet-A combustion,” *Applied Physics B*, vol. 129, no. 5, Apr. 2023, doi: <https://doi.org/10.1007/s00340-023-08015-w>.
117. R. Yuan *et al.*, “Measurement of black carbon emissions from multiple engine and source types using laser-induced incandescence: sensitivity to laser fluence,” *Atmospheric Measurement Techniques*, vol. 15, no. 2, pp. 241–259, Jan. 2022, doi: <https://doi.org/10.5194/amt-15-241-2022>.
118. M. Ihalainen *et al.*, “Design and validation of an air-liquid interface (ALI) exposure device based on thermophoresis,” *Aerosol Science and Technology*, vol. 53, no. 2, pp. 133–145, Feb. 2019, doi: <https://doi.org/10.1080/02786826.2018.1556775>.
119. Hafiz M.F. Amin and W. C. Roberts, “An experimental apparatus to measure soot morphology at high pressures using multi-angle light scattering,” *Measurement Science and Technology*, vol. 30, no. 7, pp. 075902–075902, Jun. 2019, doi: <https://doi.org/10.1088/1361-6501/ab1c3f>.
120. A. Jerez, J. J. Cruz Villanueva, L. F. Figueira da Silva, R. Demarco, and A. Fuentes, “Measurements and modeling of PAH soot precursors in coflow ethylene/air laminar diffusion flames,” *Fuel*, vol. 236, pp. 452–460, Jan. 2019, doi: <https://doi.org/10.1016/j.fuel.2018.09.047>.